nature geoscience

ARTICLES

https://doi.org/10.1038/s41561-022-00989-0

Rewetting global wetlands effectively reduces major greenhouse gas emissions

Junyu Zou[1], Alan D. Ziegler[2], Deliang Chen[3], Gavin McNicol[4], Philippe Ciais[5,6], Xin Jiang[1], Chunmiao Zheng[1,7], Jie Wu[1,8], Jin Wu[9,10], Ziyu Lin[1,9], Xinyue He[1,11], Lee E. Brown[12], Joseph Holden[12], Zuotai Zhang[1], Sorain J. Ramchunder[13], Anping Chen[14] and Zhenzhong Zeng[1]✉

Carbon and nitrogen losses from degraded wetlands and methane emissions from flooded wetlands are both important sources of greenhouse gas emissions. However, the net-exchange dependence on hydrothermal conditions and wetland integrity remains unclear. Using a global-scale in situ database on net greenhouse gas exchanges, we show diverse hydrology-influenced emission patterns in CO_2, CH_4 and N_2O. We find that total CO_2-equivalent emissions from wetlands are kept to a minimum when the water table is near the surface. By contrast, greenhouse gas exchange rates peak in flooded and drained conditions. By extrapolating the current trajectory of degradation, we estimate that between 2021 and 2100, wetlands could result in greenhouse gas emissions equivalent to around 408 gigatons of CO_2. However, rewetting wetlands could reduce these emissions such that the radiative forcing caused by CH_4 and N_2O is fully compensated by CO_2 uptake. As wetland greenhouse gas budgets are highly sensitive to changes in wetland area, the resulting impact on climate from wetlands will depend on the balance between future degradation and restoration.

Wetlands have continuously accumulated organic carbon since the Last Glacial Maximum[1], forming a dense carbon pool that stores over one-third of global soil organic carbon in only 6% of the total land area[2,3]. Alarmingly, since the Industrial Revolution, more than half of wetlands have been degraded by anthropogenic activities, including drainage, deforestation, afforestation, agricultural expansion, urbanization and climate change[4–8]. A phenomenon commonly associated with wetland degradation is the lowering of the water table, which exposes carbon pools above the water table to decomposition and releases CO_2 while simultaneously altering the natural exchange of other greenhouse gases (GHGs) including methane (CH_4) and nitrous oxide (N_2O)[9–11]. Given that degraded wetlands are important sources of GHG emissions to the atmosphere[11–14], there is a critical need not only to determine the impact of widespread wetland degradation on GHG exchanges, but also to assess the potential for wetland restoration in reducing GHG emissions.

Fluxes of CO_2, CH_4 and N_2O in wetlands are mediated by the water level relative to the surface[9,15,16]. Electron acceptor limitation in the soils of saturated wetlands is favourable to the production of methane[17,18], forming the world's largest natural source of CH_4 emissions[12]. Meanwhile, substantial CO_2 is consumed through photosynthesis by wetland vegetation; and the anaerobic conditions reduce the decomposition of organic carbon, generating a major terrestrial carbon sink over long timescales[1–3,19,20]. By contrast, the degradation of wetlands, either through drainage or desiccation, exposes stored organic matter to aerobic decomposition, resulting in the emission of CO_2 and N_2O to the atmosphere[11,15,16,21]. Previously, the relationship between GHG emissions and the water table in wetlands has been examined for only one or two GHGs[22], and for one single wetland category (for example, managed peatland[14,23,24]) or various wetland categories at local scales[11,25,26]. Lacking is a global assessment involving the three main GHGs to guide the development of effective climate change mitigation strategies and to inform the potential to restore the functioning of wetland ecosystems across moisture and temperature regimes worldwide.

We address this issue by building a global database containing in situ observations of exchange rates of GHGs for wetlands, drawn from 3,704 site-year records (Extended Data Fig. 1; refer to Methods for details). Each record contains data on wetland environmental conditions and flux information that allows quantitative assessments of the net fluxes of CO_2, CH_4 and N_2O under various wetness conditions. The reported details of the environmental conditions from each site-year record allow us to perform a new multi-gas assessment for a variety of wetland types and moisture regimes worldwide. In doing so, we classify the wetness condition of each site-year in the growing season into one of six categories that are related to the water table/level (WTL) depth below (negative number) and above (positive) the surface: WTL−3, ≤−70 cm; WTL−2, −70 cm < WTL−2 ≤ −50 cm; WTL−1, −50 cm < WTL−1 ≤ −30 cm; WTL0, −30 cm < WTL0 ≤ −5 cm; WTL1, −5 cm < WTL1 ≤ 40 cm; and WTL2, >40 cm. We illustrate differences related to temperature regimes by assessing responses across three climate zones (boreal, temperate and tropical; defined by thresholds of multiyear-average surface air temperature).

[1]School of Environmental Science and Engineering, Southern University of Science and Technology, Shenzhen, China. [2]Faculty of Fisheries Technology and Aquatic Resources, Mae Jo University, Chiang Mai, Thailand. [3]Regional Climate Group, Department of Earth Sciences, University of Gothenburg, Gothenburg, Sweden. [4]Department of Earth and Environmental Science, University of Illinois Chicago, Chicago, IL, USA. [5]Laboratoire des Sciences du Climat et de l'Environnement (LSCE), CEA CNRS UVSQ, Gif Sur Yvette, France. [6]The CYPRUS Institute, Nicosia, Cyprus. [7]EIT Institute for Advanced Study, Ningbo, Zhejiang, China. [8]Department of Geoscience and Natural Resource Management, University of Copenhagen, Copenhagen, Denmark. [9]School of Biological Sciences and Institute for Climate and Carbon Neutrality, The University of Hong Kong, Hong Kong, China. [10]State Key Laboratory of Agrobiotechnology, The Chinese University of Hong Kong, Hong Kong, China. [11]School of Earth and Environment, University of Leeds, Leeds, UK. [12]water@leeds, School of Geography, University of Leeds, Leeds, UK. [13]Singapore Botanic Gardens, National Parks Board, Singapore, Singapore. [14]Department of Biology and Graduate Degree Program in Ecology, Colorado State University, Fort Collins, CO, USA. ✉e-mail: zengzz@sustech.edu.cn

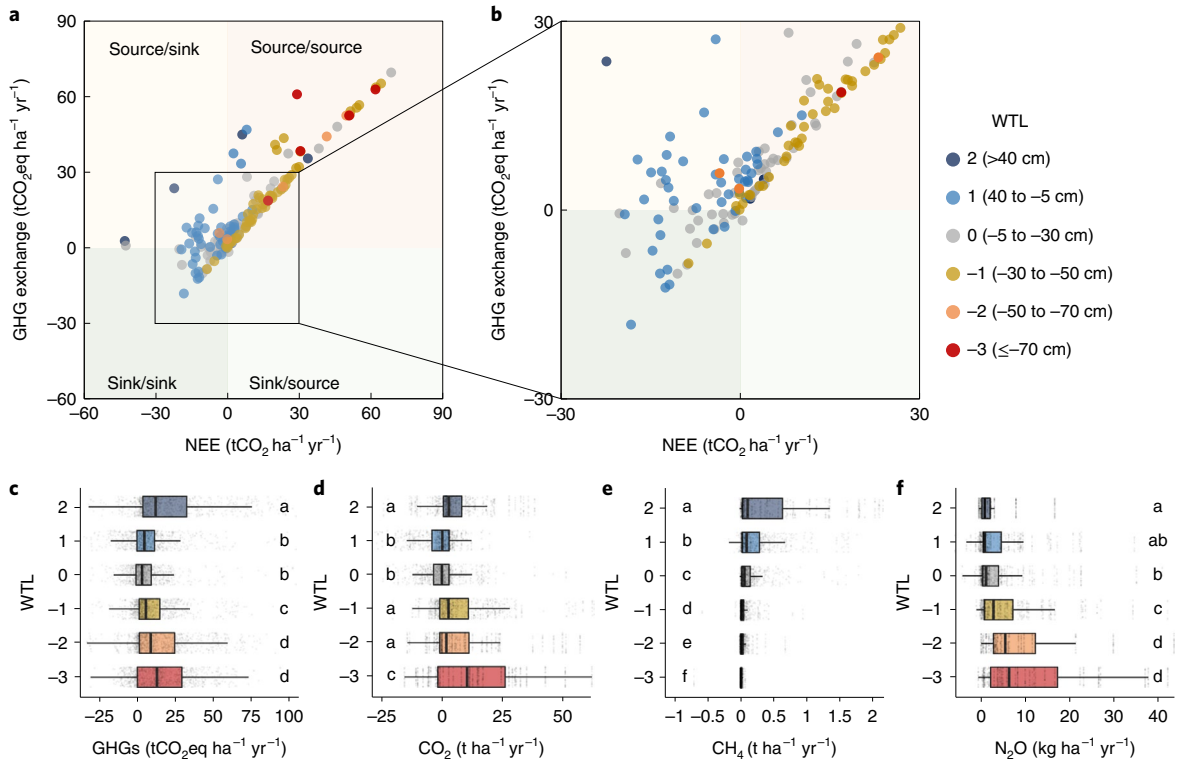

Fig. 1 | WTL effects on global wetland NEE and total GHG emissions. a, Relationship between NEE and sum of three GHG (CO_2, CH_4 and N_2O) net fluxes in different WTLs, drawn from 174 site-year records that reported three GHGs. **b**, NEE, CH_4, N_2O and sum of three net fluxes for different WTL conditions. **c**–**f**, Total (**c**) and individual (CO_2 (**d**), CH_4 (**e**), N_2O (**f**)) GHG fluxes for the six different WTLs considered. Points in each box are sampled from the original dataset (3,672 site-year records total) with 1,000 bootstraps. Different letters in the boxes indicate significant differences ($P < 0.01$) between various WTLs based on nonparametric Wilcoxon signed-rank tests. Bold vertical lines show the median; boxes indicate the middle two quartiles; horizontal lines indicate the non-outlier range. Note that *x* axes have been truncated for enhanced readability.

The nonlinear hydrothermal influence on GHG exchange

We call the CO_2 net-exchange flux at the water/land–atmosphere interface as net ecosystem exchange (NEE) (equation (1); positive/negative values indicate GHG sources/sinks). Through establishing relationships between NEE and the total GHG flux (sum of CO_2, CH_4 and N_2O in CO_2-equivalent (CO_2eq)) based on the records containing complete data, we observe the following: (1) almost all (173 of 174) records show the total GHG flux values exceed NEE for the same site-year, and (2) the differences between the NEE and total GHG flux are highly dependent on moisture conditions (Fig. 1a,b). These results indicate clearly that the wetness regulation pattern for CH_4 or N_2O emissions is different from that of CO_2 (ref. [27]). By mapping the distribution of wetness control for the three GHGs for various types of wetlands (inter alia bogs, fens, marshes, swamps, floodplain and water bodies; Methods), we identify nonlinear (parabolic) exchange patterns for NEE and the sum of GHGs and opposing monotonic patterns for CH_4 and N_2O (Fig. 1c–f and Extended Data Figs. 2a,b, 3b and 4a,b). Maximum emission of CH_4 occurs when flooded wetlands have water levels well above the soil surface (WTL2; water level > 40 cm), and the minimum occurs when the water table is well below the surface of the wetland (WTL–2 and WTL–3; water table ≤ –50 cm), indicative of a drained or desiccated state. By contrast, the highest emissions of N_2O occur during dry conditions (WTL–3), and the lowest occur in flooded conditions (WTL2). Emissions of CO_2 exhibit relative extremes for both high water-level and low water-table conditions (Fig. 1d and Extended Data Fig. 4a).

These hydrology-dependent emission patterns are in line with the expectation that CH_4 is produced in the anaerobic conditions that are associated with waterlogged soils[21,28]. Lower emissions of N_2O occur during flooded conditions because facultative anaerobic denitrifying bacteria reduce N_2O to N_2 in the oxygen-depleted water column[21,29]. As the water table falls below the soil surface, aerobic decomposition of organic matter results in an increase in CO_2 emissions[11,15,21]. As expected, the highest CO_2 emission was observed in WTL–3, where the water table is lower than 70 cm (Fig. 1d and Extended Data Fig. 4a). The relatively high CO_2 emissions observed in wetlands under flood conditions (WTL2) are probably driven by the lateral movement of organic matter across the landscape, the leaching of organic carbon into a dissolved state and subsequent oxidation by heterotrophs[30,31]. Finally, the lowest emission of the sum of all three GHGs (CO_2, CH_4 and N_2O) occurs when the water table is near the ground surface (WTL0; ranging from –30 cm to –5 cm), with near zero emissions. This nonlinear wetness pattern is in agreement with the recent report by ref. [24], which studied only selected peatland sites and did not incorporate N_2O (Extended Data Fig. 2a,b).

The parabolic pattern in GHG flux varies across boreal, temperate and tropical regimes (Fig. 2 and Extended Data Fig. 3b), demonstrating that climate influences the dependency of wetland GHG emissions on the wetness regime. The net GHG flux in each temperature regime tends to be approximately neutral when the water table is near the ground surface, although it requires higher WTL (–5 to 40 cm) to approach GHG equilibrium for the tropical sites (Fig. 2c and Extended Data Table 1). Using the empirical GHG exchange rates in the WTL2 group for different temperature regimes (Methods), we estimate the annual GHG emissions from global water bodies (lakes and reservoirs) to be 1.0 $GtCO_2\,yr^{-1}$ and 127.5 $TgCH_4\,yr^{-1}$, which is similar to the previous reports[32,33] of 1.2 $GtCO_2\,yr^{-1}$ and 175.2 $TgCH_4\,yr^{-1}$ (Supplementary Fig. 1). In addition, we estimate the CH_4 emissions from natural

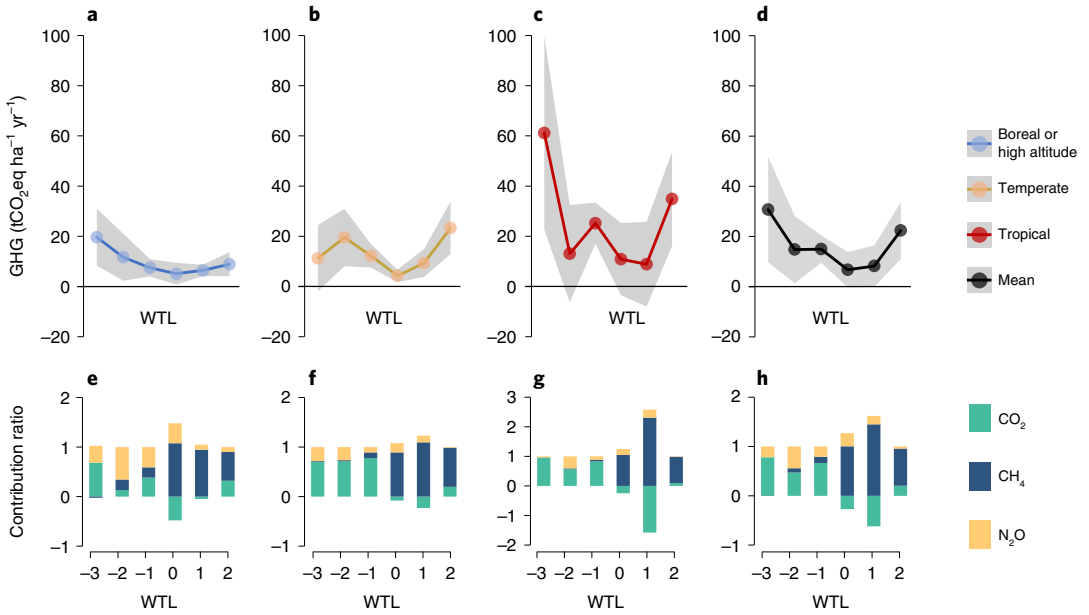

Fig. 2 | Nonlinear hydrothermal influence on GHG exchange. a–c, Dependency of GHG emissions in boreal (long-term average air temperature <4 °C) (**a**), temperate (long-term average air temperature 4–17 °C) (**b**) and tropical (long-term average air temperature >17 °C) (**c**) regions on WTL and climate. **d**, The 'mean' groups are calculated from equilateral weighted averages in each climate regime. Dots and shadows represent mean ± 1.96 SEs. **e–h**, Contribution ratios of NEE, CH_4 and N_2O to the sum of three GHG net fluxes in the three climatic regions (boreal (**e**), temperate (**f**) and tropical (**g**)) and the mean (**h**).

freshwater wetlands to be 144.4 Tg yr^{-1}, corresponding well with the 148.6 $TgCH_4$ reported by ref. [12]. Furthermore, the GHG emissions per area for wetlands with a low water table (WTL ≤ −70 cm) are 19.7 and 11.2 $tCO_2eq\,ha^{-1}\,yr^{-1}$ for boreal and temperate regimes, respectively. These values are consistent with both ref. [24] (17.60 $tCO_2eq\,ha^{-1}\,yr^{-1}$ in the case of −70 cm water level) and ref. [13], who determined the drainage-related GHG emission rates for boreal and temperate zones (16.1 $tCO_2eq\,ha^{-1}\,yr^{-1}$). These validated empirical values in the nonlinear relationship between WTL and GHG emissions then represent a novel opportunity to assess the global GHG emissions resulting from wetland degradation.

GHG emissions from wetland degradation

We evaluate past and future scenarios of wetland degradation by integrating the natural Wetland Extent Trends (WET) index[4,5] (Supplementary Fig. 2) with the Global Lakes and Wetlands Database[34] (GLWD). We assess the historical emissions from degraded wetlands at the global scale on the basis of GHG intensities at low and deep water-table conditions, which reflect wetland drainage/desiccation (WTL–3: ≤−70 cm; Extended Data Table 1 and Supplementary Fig. 3). Over the past 71 years (1950–2020), 46.22% of global wetlands have been degraded (4.85 Mkm^2), releasing 276.4 ± 175.5 $GtCO_2eq$ (95% confidence interval of GHG emissions) to the atmosphere (Fig. 3a and Extended Data Table 2). Russia, Brazil and Canada were the largest emitters because of their vast wetland areas with a high density of soil organic carbon, contributing to nearly one-half of global wetland GHG emissions: 18.6%, 15.1% and 14.6%, respectively (Figs. 3b and 4a and Extended Data Fig. 5a).

Following a history-derived, business-as-usual scenario for the future, we project that continued wetland degradation (7.76 Mkm^2, 74.0%) would release an estimated total of 407.9 ± 251.5 $GtCO_2eq$ into the atmosphere from 2021 to the end of the twenty-first century (Fig. 4b). Of these, 155.6 $GtCO_2eq$ (38.1%) will be emitted from freshwater marsh and floodplain and 96.7 $GtCO_2eq$ (23.7%) from peatlands, with the latter emitting an average of 1.21 Gt yr^{-1}, which is consistent with 1.32 Gt yr^{-1} or 1 Gt yr^{-1} reported by ref. [14] and ref. [23], respectively. Carbon dioxide would contribute the highest emissions: 306.1 ± 159.4 Gt (Extended Data Fig. 6 and Extended Data Table 2). Regionally, 71.1%, 4.6% and 24.3% of the GHG emissions would be from boreal, temperate and tropical regions, respectively. The estimate for the tropics is lower than that reported by ref. [13] because we consider the depletion of the carbon pool during 2021–2100 (Extended Data Fig. 7). Furthermore, we recognize the potential for strong, positive climate feedback in boreal areas stemming from the loss of substantial carbon storage in the future[11,35].

Emissions reduction potential under rewetting scenarios

To explore the potential for reducing GHG release from degraded wetlands, we consider two peak clipping schemes based on the rewetting of all degraded wetlands (ALL) and rewetting wetlands that contain only high organic carbon stocks (high-OCS) (Methods and Supplementary Fig. 3). We find that of a total of 4.85 Mkm^2 of degraded wetlands until 2020, fewer than half (2.02 Mkm^2) were still emitting GHGs, and the remaining 2.83 Mkm^2 were completely degraded (Supplementary Fig. 4). In the case of the latter, the soil carbon pool limits the duration for which GHGs are potentially emitted from ecosystems[36,37]. We then estimate that a widespread rewetting of degraded wetlands, with restoration rates of the same magnitude as the historical degradation rates, can potentially reduce GHG emissions by 248.7 ± 154.6 $GtCO_2eq$ (ALL rewetting scenario) and 156.4 ± 94.2 $GtCO_2eq$ (high-OCS scenario) by 2100 (Fig. 4c and Extended Data Table 2). The latter contribution was mainly from freshwater marshes and floodplains (48.6%) and peatlands (38.2%). The reduction of emissions from peatlands is an average 0.75 $GtCO_2eq\,yr^{-1}$, consistent with 0.5 Gt yr^{-1} reported by ref. [24] based on the 'optimal rewetting' scenario in which 65% of peat is under cropland and grassland (0.77 Gt in 100% peat). The corresponding CO_2 reductions are 192.9 ± 104.4 Gt (accounting for 77.6% of the sum of the three GHGs at 248.7 $GtCO_2eq$) and 107.0 ± 48.7 Gt (68.4%), respectively, for the two scenarios. Although the area proportion of high-OCS to ALL wetlands is only

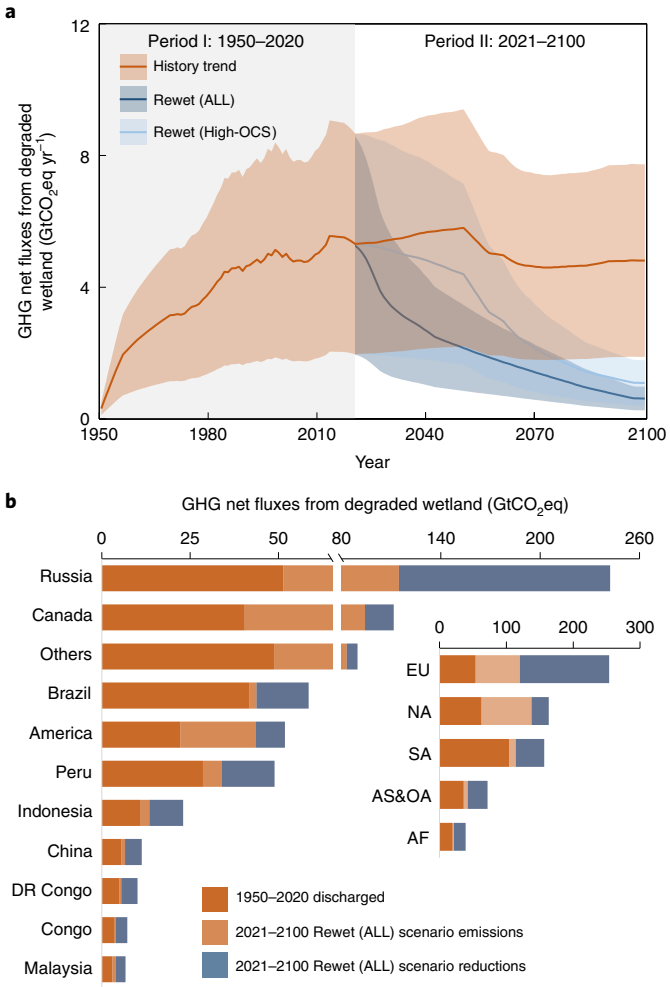

Fig. 3 | GHG emissions from degraded wetlands under different scenarios. **a**, Time series of GHG emissions from degraded wetlands under three scenarios since 1950. The emissions are constrained by natural WET index and soil organic carbon pool. 'History trend' is history-derived scenario. 'Rewet (ALL)' and 'Rewet (high-OCS)' are based on the rewetting restoration of all and only high organic carbon stock wetlands, respectively. **b**, GHG net flux from degraded wetlands in main countries and continents over different periods. 'Others' refers to the sum of GHGs from countries that were not in the top ten of GHG emitters. EU, Europe; NA, North America; SA, South America; AS&OA, Asia and Oceania; AF, Africa.

42.9% (−0.92 + 2.92 Mkm² versus 1.34 + 2.92 Mkm², Supplementary Fig. 4), the GHG emissions reduction potential is as high as 62.9% (156.4 $GtCO_2eq$ versus 248.7 $GtCO_2eq$) owing to the differences in the higher carbon density.

These projections are presumed to consider the effects of various types of wetlands and a changing climate. The duration of potential degradation related to GHG emissions from wetlands is constrained by the initial carbon pool and degradation rate (equation (4) and Supplementary Fig. 5), which vary according to wetland type and the climate regime. However, in our extension of this assessment to the future, we assume the effect of climate change will be negligible on emission rates, although there would be an unknown additional climate effect. We base this assumption on the similarity in GHG emissions rates between temperate and boreal regions for drained conditions (WTL–3: ≤−70 cm) (Fig. 2a,b and Extended Data Table 2). The similarity suggests emissions in cold regions would not change greatly with the magnitude of anticipated warming. Although the same comparison applied to the temperate versus tropical wetlands indicates a non-negligible impact of warming, the overall impact should be limited because of the low proportion of total emissions from temperate wetlands (4.6%; Extended Data Fig. 7). By contrast, emissions of GHGs in the tropics would probably be sufficient to deplete the carbon pool before 2100 (Extended Data Fig. 7a,d). Another issue of consideration is the effect that individual wetland categories would have on the effectiveness of the rewetting measures. However, there are consistent GHG exchange rates across various wetland categories (Supplementary Fig. 6a–f) that are similar to the sum exchange of GHGs across different climate regimes (for example, WTL0; Fig. 2a–c and Extended Data Table 2), although for which CO_2 and CH_4 fluxes vary significantly (Supplementary Fig. 7a–c).

A general limitation in our assessment stems from the natural WET index being produced at an intercontinental scale rather than at a local scale[4,5]. This limitation prevents the development of a more detailed assessment of the GHG budgets associated with wetland degradation and/or restoration. In addition, we could not consider fire disturbances for wet versus dry conditions[38,39] or the response of substratum over one metre deep. Thus, our estimated GHG emissions from degraded wetlands may be conservative, and the GHG-reduction potential of rewetting programmes is likely to be underestimated. Nevertheless, our estimated annual emissions from degraded wetlands for CO_2 and N_2O, or from whole natural freshwater wetlands for CH_4, are significantly correlated with their respective annual growth rates in atmospheric concentration[40] during the past three decades ($P < 0.05$; Extended Data Fig. 8; more details in Wetland GHG budgets and inter-annual atmospheric GHG growth rates), supporting the utility of our method of integrating the natural WET index with the empirical GHG emission rates. Furthermore, the magnitudes of the estimated CO_2, CH_4 and N_2O emissions from the wetlands, equalling 10.8 ± 6.2%, 38.5 ± 16.7% and 30.5 ± 19.4%, respectively, of the anthropogenic sources[12,41,42], are in line with the aforementioned correlations.

Despite uncertainties, we find that wetland rewetting is an effective nature-based solution to mitigate climate change. The rewetting ALL scenario and the high-OCS scenario require preserving or restoring 4.26 Mkm² and 2 Mkm² areas of degraded wetlands, respectively, compared with the business-as-usual scenario derived from historical trends (Supplementary Fig. 4). The two rewetting scenarios can reduce GHG emissions by 583.8 $tCO_2eq\,ha^{-1}$ and 782 $tCO_2eq\,ha^{-1}$, respectively. The potential of GHG reduction from wetland restoration at this scale is higher than that from the rehabilitation of other types of ecosystems, for example, forest regrowth equivalent to 394.2 $tCO_2\,ha^{-1}$ across 6.78 Mkm² of afforestation under the 'maximum' scenario, or 504.3 $tCO_2\,ha^{-1}$ across 3.49 Mkm² under the 'national commitments' scenario[43]. At present, Indonesia, Europe and North America have already shown the benefits of raising water tables by both artificial and natural means[44–47]. In cases where the water table is lowered by groundwater extraction, water conservancy measures may be needed to regulate water use—and the potential negative impacts of doing so should be balanced[48,49].

Conclusion

In conclusion, the nonlinear thermal-wetness influence on wetland GHG fluxes, whereby a near-surface water table produces near-neutral GHG flux across broad temperature gradients, suggests that rewetting wetlands is an effective nature-based solution to mitigate climate change. A volume equivalent to 10% of anthropogenic CO_2 emissions could be reduced through wetland restoration. By quantifying the impact of natural wetland area changes on multiple GHG budgets under several scenarios, we provide primary information for nature-based solutions predicated on wetland restoration for countries aiming to achieve net-zero emission targets[50]. Furthermore, we emphasize the enormous loss of organic matter and GHG emissions from over half of the global wetland ecosystems

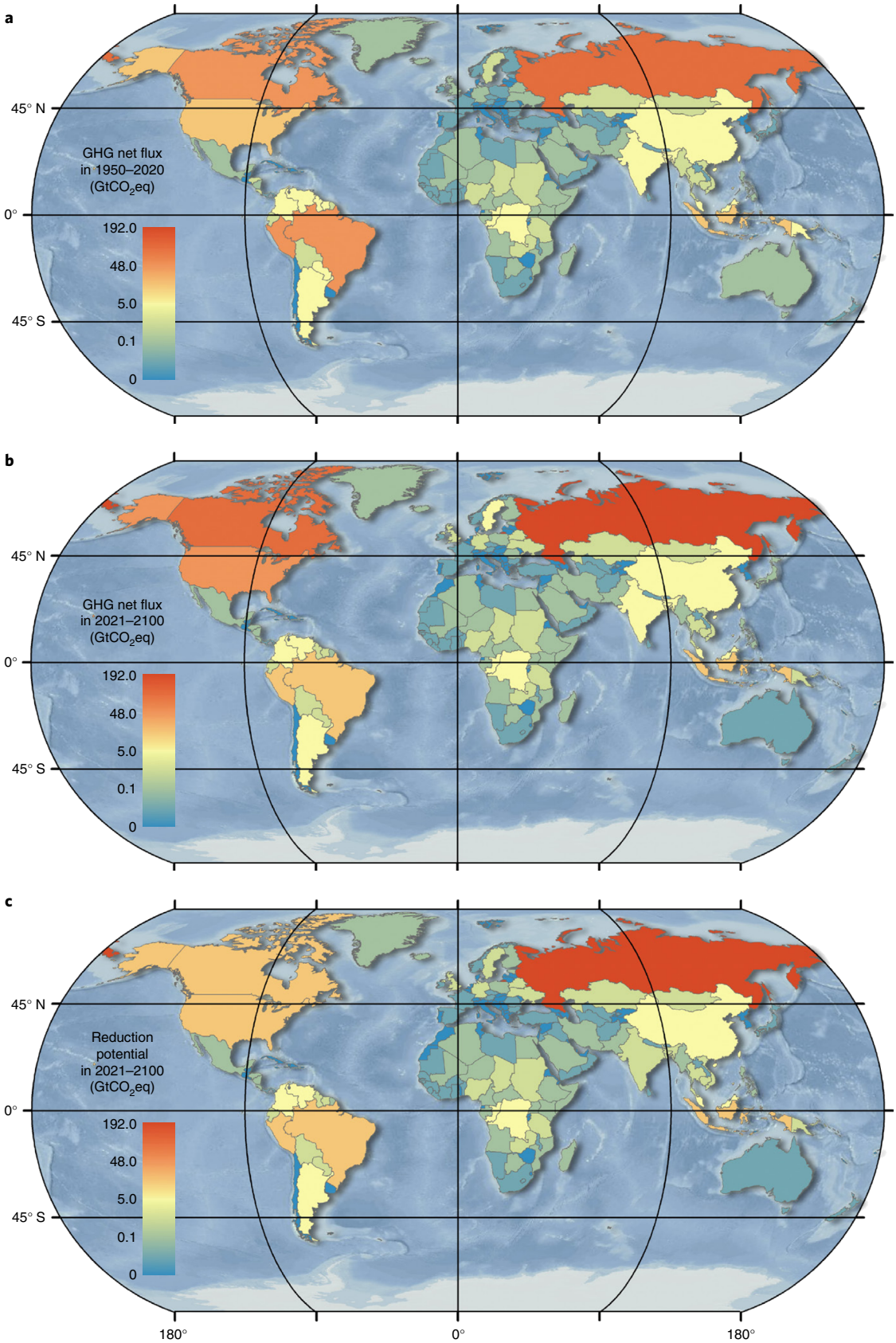

Fig. 4 | Spatial pattern of the GHG emissions owing to wetland degradation and reduction potential via rewetting wetlands. a,**b**, The GHG emissions owing to wetland degradation under history-driven scenario in 1950–2020 (**a**) and under history-driven, business-as-usual scenario in 2021–2100 (**b**). (**c**) The reduction potential under Rewet (ALL) scenario in 2021–2100.

due to drying. Finally, we show that future emissions from these sources can be mitigated or even halved by rewetting wetlands to a near-surface water table.

Online content

Any methods, additional references, Nature Research reporting summaries, source data, extended data, supplementary information, acknowledgements, peer review information; details of author contributions and competing interests; and statements of data and code availability are available at https://doi.org/10.1038/s41561-022-00989-0.

Received: 9 August 2021; Accepted: 10 June 2022;
Published online: 28 July 2022

References

1. Lindgren, A., Hugelius, G. & Kuhry, P. Extensive loss of past permafrost carbon but a net accumulation into present-day soils. *Nature* **560**, 219–222 (2018).
2. Nichols, J. E. & Peteet, D. M. Rapid expansion of northern peatlands and doubled estimate of carbon storage. *Nat. Geosci.* **12**, 917–921 (2019).
3. Bridgham, S. D. et al. The carbon balance of North American wetlands. *Wetlands* **26**, 889–916 (2006).
4. Dixon, M. J. R. et al. Tracking global change in ecosystem area: the wetland extent trends index. *Biol. Conserv.* **193**, 27–35 (2016).
5. Darrah, S. E. et al. Improvements to the Wetland Extent Trends (WET) index as a tool for monitoring natural and human-made wetlands. *Ecol. Indic.* **99**, 294–298 (2019).
6. Asselen, S. et al. Drivers of wetland conversion: a global meta-analysis. *PLoS ONE* **8**, e81292 (2013).
7. Davidson, N. C. How much wetland has the world lost? Long-term and recent trends in global wetland area. *Mar. Freshw. Res.* **65**, 934–941 (2014).
8. Galatowitsch, S. M. in *The Wetland Book II: Distribution, Description, and Conservation* (eds Finlayson, C.M. et al.) 359–367 (Springer, 2018).
9. Limpert, K. E. et al. Reducing emissions from degraded floodplain wetlands. *Front. Environ. Sci.* **8**, 8 (2020); https://doi.org/10.3389/fenvs.2020.00008
10. Laine, J. et al. Effect of water-level drawdown on global climatic warming: northern peatlands. *AMBIO* **25**, 179–184 (1996).
11. Ise, T. et al. High sensitivity of peat decomposition to climate change through water-table feedback. *Nat. Geosci.* **1**, 763–766 (2008).
12. Saunois, M. et al. The global methane budget 2000–2017. *Earth. Syst. Sci. Data* **12**, 1561–1623 (2020).
13. Leifeld, J. et al. Intact and managed peatland soils as a source and sink of GHGs from 1850 to 2100. *Nat. Clim. Change* **9**, 945–947 (2019).
14. Günther, A. et al. Prompt rewetting of drained peatlands reduces climate warming despite methane emissions. *Nat. Commun.* **11**, 1644 (2020).
15. Hooijer, A. et al. Subsidence and carbon loss in drained tropical peatlands. *Biogeoscience* **9**, 1053–1071 (2012).
16. Prananto, J. A. et al. Drainage increases CO_2 and N_2O emissions from tropical peat soils. *Glob. Change Biol.* **26**, 4583–4600 (2020).
17. Jauhiainen, J. et al. Carbon dioxide and methane fluxes in drained tropical peat before and after hydrological restoration. *Ecology* **89**, 3503–3514 (2008).
18. Bridgham, S. D. et al. Methane emissions from wetlands: biogeochemical, microbial, and modeling perspectives from local to global scales. *Glob. Change Biol.* **19**, 1325–1346 (2013).
19. Schuldt, R. et al. Modelling Holocene carbon accumulation and methane emissions of boreal wetlands—an Earth system model approach. *Biogeosciences* **10**, 1659–1674 (2012).
20. McNicol, G. et al. Effects of seasonality, transport pathway, and spatial structure on greenhouse gas fluxes in a restored wetland. *Glob. Change Biol.* **23**, 2768–2782 (2017).
21. Yu, K. et al. Redox window with minimum global warming potential contribution from rice soils. *Soil Sci. Soc. Am. J.* **68**, 2086–2091 (2004).
22. Huang, Y. et al. Tradeoff of CO_2 and CH_4 emissions from global peatlands under water-table drawdown. *Nat. Clim. Change* **11**, 618–622 (2021).
23. Ojanen, P. & Minkkinen, K. Rewetting offers rapid climate benefits for tropical and agricultural peatlands but not for forestry-drained peatlands. *Glob. Biogeochem. Cycles* **34**, e2019GB006503 (2020).
24. Evans, C. D. et al. Overriding water table control on managed peatland greenhouse gas emissions. *Nature* **593**, 548–552 (2021).
25. Strack, M., Keith, A. M. & Xu, B. Growing season carbon dioxide and methane exchange at a restored peatland on the Western Boreal Plain. *Ecol. Eng.* **64**, 231–239 (2014).
26. Karki, S. et al. Carbon balance of rewetted and drained peat soils used for biomass production: a mesocosm study. *Glob. Change Biol. Bioenergy* **8**, 969–980 (2016).
27. Whiting, G. J. & Chanton, J. P. Greenhouse carbon balance of wetlands: methane emission versus carbon sequestration. *Tellus B* **53**, 521–528 (2001).
28. Moore, T. R. et al. A multi-year record of methane flux at the Mer Bleue Bog, Southern Canada. *Ecosystems* **14**, 646–657 (2011).
29. Zhu, X. et al. Ammonia oxidation pathways and nitrifier denitrification are significant sources of N_2O and NO under low oxygen availability. *Proc. Natl Acad. Sci. USA* **110**, 6328–6333 (2013).
30. Cole, J. J. et al. Plumbing the global carbon cycle: integrating inland waters into the terrestrial carbon budget. *Ecosystems* **10**, 171–184 (2007).
31. Holgerson, M. A. & Raymond, P. A. Large contribution to inland water CO_2 and CH_4 emissions from very small ponds. *Nat. Geosci.* **9**, 222–226 (2016).
32. Raymond, P. A. et al. Global carbon dioxide emissions from inland waters. *Nature* **503**, 355–359 (2013).
33. Rosentreter, J. A. et al. Half of global methane emissions come from highly variable aquatic ecosystem sources. *Nat. Geosci.* **14**, 225–230 (2021).
34. Lehner, B. & Döll, P. Development and validation of a global database of lakes, reservoirs and wetlands. *J. Hydrol.* **296**, 1–22 (2004).
35. Schuur, E. A. et al. The effect of permafrost thaw on old carbon release and net carbon exchange from tundra. *Nature* **459**, 556–559 (2009).
36. Delgado-Baquerizo, M. et al. Climate legacies drive global soil carbon stocks in terrestrial ecosystems. *Sci. Adv.* **3**, e1602008 (2017).
37. Hengl, T. et al. SoilGrids250m: global gridded soil information based on machine learning. *PLoS ONE* **12**, e0169748 (2017).
38. Walker, X. J. et al. Increasing wildfires threaten historic carbon sink of boreal forest soils. *Nature* **572**, 520–523 (2019).
39. Baird, A. J. et al. Validity of managing peatlands with fire. *Nat. Geosci.* **12**, 884–885 (2019).
40. Ritchie, H., Roser, M. & Rosado, P. *CO_2 and GHG Emissions: Atmospheric Concentrations* (Our World in Data, 2020); https://ourworldindata.org/atmospheric-concentrations#citation
41. Friedlingstein, P. et al. Global carbon budget 2019. *Earth Syst. Sci. Data* **11**, 1783–1838 (2019).
42. Tian, H. et al. A comprehensive quantification of global nitrous oxide sources and sinks. *Nature* **586**, 248–256 (2020).
43. Cook-Patton, S. C. et al. Mapping carbon accumulation potential from global natural forest regrowth. *Nature* **585**, 545–550 (2020).
44. Jaenicke, J. et al. Planning hydrological restoration of peatlands in Indonesia to mitigate carbon dioxide emissions. *Mitig. Adapt. Strateg. Glob. Change* **15**, 223–239 (2010).
45. Wohl, E. Landscape-scale carbon storage associated with beaver dams. *Geophys. Res. Lett.* **40**, 3631–3636 (2013).
46. Law, A. et al. Using ecosystem engineers as tools in habitat restoration and rewilding: beaver and wetlands. *Sci. Total Environ.* **605–606**, 1021–1030 (2017).
47. Brown, L. E. et al. Macroinvertebrate community assembly in pools created during peatland restoration. *Sci. Total Environ.* **569**, 361–372 (2016).
48. Finlayson, C. M. & Rea, N. Reasons for the loss and degradation of Australian wetlands. *Wetl. Ecol. Manage.* **7**, 1–11 (1999).
49. Liu, J. et al. Water conservancy projects in China: achievements, challenges and way forward. *Glob. Environ. Change* **23**, 633–643 (2013).
50. Rogelj, J. et al. in *Special Report on Global Warming of 1.5 °C* (eds Masson-Delmotte, V. et al.) Ch. 2 (IPCC, WMO, 2018).

Methods

In situ database of GHGs. We searched for literature through the Web of Science using the following strings: (greenhouse gases flux (greenhouse gas* OR GHG* OR carbon dioxide OR CO_2 OR net ecosystem productivity* OR NEP OR net ecosystem exchange* OR NEE OR carbon OR methane OR CH_4 OR nitrous oxide OR N_2O OR flux* OR emission* OR global warming potential OR GWP) OR (degradation* OR decline*) and wetland (wetland* OR water* OR peatland* OR bog* OR fen* OR swamp* OR mire* OR soil* OR river* OR paddy OR pool* OR floodplain* OR reservoir* OR coastal* OR saltmarsh*)). The search returned 33,835 papers after excluding those in irrelevant fields. After screening the manuscripts to ensure that the records contained measured data from field monitoring projects, 2,563 papers were manually selected, from which we read to extract the following information: (1) gas sample collection methods (this content may be missing, for example, eddy covariance method (EC) measured CO_2 and/or CH_4 fluxes without collecting gas samples) and measurement techniques; (2) time intervals and the duration of sample collection (we specified that the monitoring span during the growing season should be at least three months in temperate regions); (3) detailed site information, in particular geographic coordinates or maps that could be georeferenced, as well as topography, ecosystem type, plant species and soil carbon features. After screening, we obtained 504 papers with valid data (Supplementary Data 1). Parts of those data were extracted from figures by GetData Graph (version 2.26).

Record details. We constructed a GHG net-flux database consisting of 3,704 site-years (1,875 sites) for locations situated between 81°48′N and 78°01′S (Extended Data Fig. 1a–c) across all the continents, but mainly in Asia, Europe and North America. The sample collection method and measurement technique used in these field monitoring projects usually depended on the type of wetland and associated environmental conditions. Common collection methods included the static chamber method[51], dynamic chamber method[52] and floating chamber method[53]. Common measurement techniques involve the use of infrared gas analyser and the combination of gas chromatography with physical model methods (for example, EC[54], CO_2/CH_4-diffusivity formula[53], oxygen diffusivity formula[55] or chlorophyll-dissolved oxygen model[56]). We assume that these GHG exchange rates from peer-reviewed papers based on different sampling methods are of equivalent accuracy, although there may be differences in precision.

Nomenclature corresponding to the exchange of CO_2 between the ecosystem and the atmosphere used in various methods is diverse. The EC method generally uses a net ecosystem exchange (NEE) to characterize the flux, while the chamber method adopts the net ecosystem production approach. While a few sites measure both vertical exchange and transverse flow of GHGs[2,30], most of the sites report only the measurements of vertical fluxes. Consequently, the datasets we built describe the fluxes in the vertical direction. In cases where data were reported for the growing seasons (Extended Data Fig. 1b), we filled in the missing data using linear regression on the basis of complete data containing both growing and annual records (Supplementary Table 1). There was no significant interaction effect of climate regimes on the slope, and only a subtle effect on the intercept of the NEE regression equation for temperate zones. Therefore, we chose linear regression equations that did not consider the interaction of the climate regimes.

We used NEE to describe the net vertical exchange capacity:

$$\mathrm{NEE} = \mathrm{Re} - \mathrm{GPP} = \mathrm{Rh} - \mathrm{NPP} \quad (1)$$

where Re is ecosystem respiration, GPP is gross primary productivity, Rh is heterotrophic respiration and NPP is net primary productivity. Positive values of NEE indicate carbon loss via CO_2 emission to the atmosphere, whereas negative values indicate carbon gain because CO_2 is retained/stored in the ecosystem.

Building on equation (1), we calculated the total flux of three GHGs—carbon dioxide, methane and nitrous oxide—as

$$\mathrm{GHGs} = \mathrm{NEE} + 34\mathrm{CH_4} + 298\mathrm{N_2O} \quad (2)$$

where CO_2 is substituted by NEE. Units for all terms are $kgCO_2eq\,ha^{-1}\,yr^{-1}$; the weights 34 and 298 are global warming potential (GWP) for CH_4 and N_2O to CO_2eq by weights on a 100 yr perspective with feedbacks considered[57], respectively.

Uncertainty is represented by incorporating 95% confidence intervals (CIs):

$$\mathrm{GHGs\_CI} = \mathrm{NEE\_CI} + 34\mathrm{CH_4\_CI} + 298\mathrm{N_2O\_CI} \quad (3)$$

where the CI of three GHGs on the right side of equation (3) originate from within groups, whereby uncertainties in empirical GHG emission rates are obtained for 18 groups, including 6 WTL categories × 3 climatic zones.

Wetland categories. The majority of the records collected in this study were measured in natural wetlands, including bogs, fens, mires, swamps, marshes and floodplains; we also considered water bodies as extensions. We distinguished peatlands from non-peatlands on the basis of the soil organic layer thickness (peatlands: ≥40 cm)[58] to explore the influence of soil organic matter on multi-GHG fluxes. We divided all sites into six water categories on the basis of either the water level (flooded) or the water-table height (non-flooded) relative to the surface (WTL) for three climatic regions (tropical, temperate, and boreal or high-altitude areas, using 4 °C and 17 °C as thresholds of multiyear-average annual temperature)[59]. We also treat water level as a continuous variable in Extended Data Fig. 2, using 2,318 site-year records that reported exact water levels. Unfortunately, reports with high-quality water-level records from the tropics accounted for only 7% of the total. As such, the trend for the tropics using the continuous variable approach has more uncertainty than for other climates. Therefore, we segmented all the WTL data. The WTL classes were separated by mean water table/level during the growing season due to the discontinuity of the reported hydrological records during winter at most sites. Six classes are designated: WTL–3, ≤–70 cm; WTL–2, –70 cm < WTL–2 ≤ –50 cm; WTL–1, –50 cm < WTL–1 ≤ –30 cm; WTL0, –30 cm < WTL0 ≤ –5 cm; WTL1, –5 cm < WTL1 ≤ 40 cm; and WTL2, >40 cm. Positive numbers indicate that the water level is above the surface. This classification is based on the empirical water-level critical value of the soil moisture conditions, ranging from drought to moist to near-saturated to oversaturated[60]. We used an empirical value of 40 cm water level as a threshold to classify high water levels as they usually inhibit the establishment of emergent plants. We defined the start/end of a growing season as the time when the daily mean temperature for five continuous days was above/below 5 °C for the first time[61].

We extracted the global natural wetland map from the GLWD level 3 (GLWD-3, classes 4, 5, 8–12)[34], which provides reliable areas of global wetlands, with tropical peatlands distinguished[62–64]. Its classification of wetlands also agrees with most records in the literature we selected. Gridded long-term mean annual air temperature was calculated using the monthly data from the latest European Centre for Medium-Range Weather Forecasts reanalysis (ERA5 (ref. [65])) for 1978–2018. Gridded wetland soil OCS was obtained from SoilGrids[37], which indicates that natural freshwater wetlands cover 7.66 million km^2 and store 329.5 GtC in the upper one metre of the soil (Extended Data Table 2). The proportion of wetlands in boreal, temperate and tropical regions are 45.8%, 10.8% and 43.4%, respectively.

Dynamic area of wetlands under three scenarios. Means and 95% CIs of GHG net fluxes in WTL–3 (≤–70 cm) for different climatic zones were used as the emission potential from degraded wetlands (Extended Data Fig. 2b and Extended Data Table 1). We employed the mean OCS for each wetland category in each country as a constraint and then calculated the duration potential (Supplementary Fig. 5) of soil carbon efflux from degraded wetlands for 21 wetland types (3 climate zones (tropical, temperate, and boreal or high-altitude zones) × 7 wetland category groups (bog, fen, mire, swamp forest, flooded forest, freshwater marsh and floodplain)) at the national scale as follows:

$$\mathrm{DP} = (\mathrm{OCS} - \mathrm{OCS_t})/\mathrm{NEE},\ \mathrm{DP} \geq 1 \quad (4)$$

We used an OCS_t (threshold) of 50 $t\,ha^{-1}$ (ref. [36]), after which an ecosystem has no potential for net CO_2 emission from the soil layer. To avoid double counting, we did not consider the other GHG exchanges of completely degraded wetlands, which have been definitely converted into farmland or pasture, and so on. These are included in the estimate of land-use and agriculture emissions by the Carbon Budget Project[35] and the Food and Agriculture Organization[66].

We rebuilt the historical trend and predicted the future wetland degradation rate at the continental scale using the natural WET index[4,5] for 1970–2015 (Supplementary Fig. 2). The WET index is a multi-source composite index to represent the proportion of wetland degradation or construction during 1970–2015 (Europe in 1970–2013). We extended the time series to 1950–1969 and 2016–2100 from regressions using the 1970–1990 and 2000–2015 data (Europe predicted by 2000–2013 due to the data restriction); these calculations are for the history-derived (history-derived) scenario. We used two wetland restoration benchmarks: one considered all wetlands (ALL) and the other involved only the high-OCS wetlands (high-OCS) (Supplementary Fig. 3). High-OCS wetlands were determined as those with a duration potential >80 yr. The total area of high-OCS wetlands worldwide is 3.29 Mkm^2, of which 34.5% are degraded. The ALL and high-OCS scenarios were both grounded on the assumption that the restoration rate of those degraded wetlands would exceed that of the historical degradation rate in all continents by 2030. Thus, before 2030, restoration proceeded at a rate equivalent to the absolute value of the degradation rate during 2000–2015 (2000–2013 for Europe). The increase stopped when the natural WET index recovered to the level in 1950 (Supplementary Fig. 2).

A completely degraded wetland was defined as having no potential for soil carbon loss, and the wetland during degradation was defined as having continuous loss of carbon and nitrogen (WTL–3) to the atmosphere. The remainder were classified as initial and rewetted wetlands. The component of dynamic wetland area under three scenarios in Supplementary Fig. 4 shows the trends of the area in three conditions during 1950–2100 (more details in Supplementary Data 1).

Supporting calculations. *Empirical GHG exchange rates.* On the basis of the empirical values (WTL0, WTL2) in the relationship between WTL and GHG emissions across different temperature regimes (Extended Data Table 1), we calculated that the GHG emissions from global water bodies (lakes and reservoirs) are 1.0 ± 0.93 $GtCO_2$ and 127.5 ± 49.4 $TgCH_4$, and CH_4 emissions from natural freshwater wetlands are 144.4 ± 67.9 Tg. These results agree with previous reports,

whose corresponding values are $1.2^{+1.91}_{-0.95}$ $GtCO_2$ (ref. [32]), 175.2 ± 81 $TgCH_4$ (ref. [33]) and 148.6 ± 15.2 $TgCH_4$ (ref. [12]), respectively (Supplementary Fig. 1).

The GHG emissions from boreal and temperate regimes in WTL–3 (≤–70 cm) are 19.7 and 11.2 $tCO_2eq\,ha^{-1}\,yr^{-1}$, respectively, which are similar to the drained-induced GHG emission factor 16.1 $tCO_2eq\,ha^{-1}\,yr^{-1}$ for boreal and temperate in ref. [13]. Furthermore, the CO_2 emission rate in the boreal regime is $13.43^{+5.48}_{-5.48}$ $tCO_2\,ha^{-1}\,yr^{-1}$, which is similar to the cultivated northern peatlands emission factor $13.2^{+0.73}_{-1.1}$ $tCO_2\,ha^{-1}\,yr^{-1}$ in ref. [67] from a process-based land surface model.

Estimation of GHG emissions from degraded wetlands under three scenarios. We estimated the changes of GHG emissions driven by the degraded wetland area and OCS in various wetland types under three scenarios (history-derived, ALL and high-OCS) and across different scales. At the national scale, countries with large OCS were the dominant emitters of GHGs, mainly CO_2. The top ten GHG emitting countries contributed to 79.6% of the total emissions in the period 1950–2020 (Fig. 3 and Extended Data Figs. 5 and 6). At the continental scale, the top two continents, South America (SA) and North America (NA), accounted for 37.7% and 22.7%, respectively. With respect to climate regime, countries in tropical and boreal regions occupied 55.4% and 39.7%, respectively, due to their potent outflow and high OCS.

In the scenario for which the historical trend continues during the period 2021–2100 (history-derived scenario), the wetland degradation area will increase to 74.0% by the end of the twenty-first century, and the induced GHGs will be enlarged by 1.48 times to 407.9 Gt (Figs. 3 and 4 and Extended Data Table 2). In addition, the present geographical pattern of outflow will change: in tropical regions, along with the loss of most soil OCS, emissions will reduce from 155.2 Gt to 99.1 Gt, while boreal regions will become the dominant emissions source, increasing from 107.9 Gt to 290.0 Gt (39.0% to 71.1%).

Under the wetland restoration scenarios for which rewetting occurs for all degraded wetlands (ALL) or only high-OCS degraded wetlands (high-OCS), the total GHG emissions could reduce by 248.7 or 156.4 Gt, respectively. The emissions reduction results mainly from the reduced GHG emissions over boreal regions. In the high-OCS scenario, CO_2 accounted for 79.2% of the global total GHG emissions (Extended Data Table 2), higher than in the ALL scenario (71.2%) and the history-derived scenario (75.0%). This finding results from a large percentage of the degraded low-OCS wetlands being distributed in the tropics but not restored in the high-OCS scenario, where the tropics contribute to the largest portion of global CO_2 emissions with the highest CO_2 outflow potential per area (Fig. 2 and Extended Data Fig. 5).

All the preceding conclusions are based on a GWP for CH_4 of 34-fold that of CO_2 by weights over a 100 yr period. We have also supplemented our assessment of emissions and reductions with a 28-fold GWP or a 45-fold sustained GWP[68,69]. The results of GHG emissions estimation show differences of +0.23% and –0.43%, respectively, compared with the history-derived scenario with a 34-fold base in 1950–2100. The estimation of GHG emissions reduction change is +0.37% and –0.67% under the rewetting ALL scenario, and +0.22% and –0.41% under the rewetting high-OCS scenario in 2020–2100, respectively.

Wetland GHG budgets and inter-annual atmospheric GHG growth rates. There are significant correlations between annual growth rates in atmospheric concentrations and changes in the wetland-induced flux for CO_2, CH_4 and N_2O in 1979–2018 ($P < 0.05$; Extended Data Fig. 8a–i; N_2O is in 1979–2016). The sum of N_2O emissions from degraded wetland and Food and Agriculture Organization agriculture-total[66] is also significantly correlated with atmospheric concentration growth rates ($P < 0.05$; note that N_2O data exclude two early extreme values in 1979 and 1982). Emissions of CO_2 from degraded wetlands are highly consistent with those from land-use changes in the Carbon Budget Project[35], with the former being ~81.4% (ranging from 64.5% to 97.5%) of the latter across 30 years. The net CH_4 emissions from degraded and from initial and rewetted wetlands both exhibited a downward trend during 1979–2018. This change may have contributed to the decline of atmospheric methane growth rates before 2005, which is reversed by the increase of emissions from other major sources (for example, agriculture[68]) since then. The evident correlations between wetland budgets and atmospheric growth of three key GHGs indicate the non-negligible impact of wetland degradation. Indeed, CO_2, CH_4 and N_2O emissions from wetlands were equal to 10.8 ± 6.2%, 38.5 ± 16.7% and 30.5 ± 19.4% of those from anthropogenic sources[12,41,42], similar to their contributions of 19%, 21% and 34% of the variation in atmospheric concentrations during 1979–2018 (Extended Data Fig. 8).

Uncertainties. *Wetland area.* Although many global wetland area products using diverse classification rules have been released[34,70–75], uncertainty remains in wetland characterizations and distribution worldwide. In particular, human-made wetlands have been increasing greatly in recent years, and natural wetlands continue to degrade[4,5,76]. The natural wetland classes (bog, fen, mire, swamp/flooded forest, freshwater marsh and floodplain) of GLWD-3 were built from the following three datasets in the 1990s: ArcWorld[77], Digital Chart of the World[78] and World Concervation Monitoring Centre[79]. We conservatively considered the area of wetlands in GLWD-3 as the background value in 1990. The GLWD-3 did not include wetlands smaller than 0.1 km^2; however, this threshold ensured that the hydrologic features and biogeochemical processes of degraded wetlands can be restored to their initial states in a short term[80].

Degradation trend of natural wetlands. Many countries lack baseline wetland inventories that allow us to accurately track the lengthy and complex degradation of natural wetlands[81]. The WET index represents area change based on over 2,000 wetland area records in long-term time series from six regions and distinguishes between human-made and natural wetland changes from 1970 to 2015. Given the differences between natural and artificial wetlands in the basal features (for example, OCS and hydrologic features) and disturbance (for example, artificial landscape and artificial nitrogen input), we considered only natural wetlands via down-scaling the natural WET index from six continents to countries and/or regions. Therefore, additional surveys and remote-sensing data would provide a more accurate assessment at a finer scale in the future.

According to the WET index, the degraded wetland areas were 4.85 Mkm^2 for 1950–2020 (46.22% of the global natural wetlands). Under a history-derived, business-as-usual scenario for the future, we projected that continued wetland degradation will reach 7.76 Mkm^2 (74.0%) by the end of the 2021–2100 period. Note that these overall estimates include those wetlands degraded not only by land-use change (for example, reclamation and draining) but also by other factors affecting the hydrological characteristics of wetlands (desiccation)[82]. For example, the peat loss to extraction or farming in Europe accounts for only 11% of European peatlands[67], but the water levels in another 50% of European peatlands are also declining, causing degradation[83].

Wetland categories. Empirical parameter generalization is based on the premise that there is no difference in emission potential across various wetland categories. Indeed, we found that, in the WTL0 group, where GHG emissions are close to neutral (Fig. 2 and Extended Data Table 1), there is almost no significant difference in GHG emissions among the main wetland categories for both tropical and temperate regimes (Supplementary Fig. 6). However, because of the lack of various types of wetlands in boreal regions (dominated by peatlands), we did not test the differences in GHG emissions across diverse categories for boreal climates. In the WTL–3 group, due to the lack of various wetland categories for comparison, we used the OCS to calculate the duration potential, which is further used to constrain the empirical parameter generalization for the estimate of the potential GHG emissions from degraded wetlands (equation (4)).

Data availability

GLDW dataset is available at http://www.wwfus.org/science/data.cfm. Soilgrids dataset is available at https://soilgrids.org. ECMWF reanalysis climate data are available at https://cds.climate.copernicus.eu/#!/home. FAOSTAT emissions database is available at http://www.fao.org/faostat/en/#data/GT. Atmospheric concentrations data are available at https://ourworldindata.org/atmospheric-concentrations. All GHG data are available in the main text or the supplementary materials. The database of global, in situ, GHG exchange information for wetlands, drawn from 3,704 site-year records, is summarized in Supplementary Data 1. Source data are provided with this paper.

Code availability

The scripts used to generate all the results are MATLAB (R2018a), R-4.1.0 and Python 2.7 based on arcpy. Analysis scripts are available at https://github.com/XiaoBai0417/Multi-greenhouse-gas-assessments.

References

51. Svensson, B. H. & Rosswall, T. In situ methane production from acid peat in plant communities with different moisture regimes in a subarctic mire. *Oikos* **43**, 341–350 (1984).
52. Waddington, J. M. & Roulet, N. T. Atmosphere–wetland carbon exchanges: scale dependency of CO_2 and CH_4 exchange on the developmental topography of a peatland. *Glob. Biogeochem. Cycles* **10**, 233–245 (1996).
53. Kling, G. W. et al. The flux of CO_2 and CH_4 from lakes and rivers in Arctic Alaska. *Hydrobiologia* **240**, 23–36 (1992).
54. Humphreys, E. R. et al. Two bogs in the Canadian Hudson Bay lowlands and a temperate bog reveal similar annual net ecosystem exchange of CO_2. *Arct. Antarct. Alp. Res.* **46**, 103–113 (2014).
55. Caffrey, J. M. Factors controlling net ecosystem metabolism in US estuaries. *Estuaries* **27**, 90–101 (2004).
56. Roberts, B. J. et al. Multiple scales of temporal variability in ecosystem metabolism rates: results from 2 years of continuous monitoring in a forested headwater stream. *Ecosystems* **10**, 588–606 (2007).
57. Myhre, G. et al. in *Climate Change 2013: The Physical Science Basis* (eds Stocker, T.F. et al.) 710–714 (Cambridge Univ. Press, 2013).
58. Glenn, A. J. et al. Comparison of net ecosystem CO_2 exchange in two peatlands in western Canada with contrasting dominant vegetation, *Sphagnum* and *Carex*. *Agric. For. Meteorol.* **140**, 115–135 (2006).

59. Bond-Lamberty, B. & Thomson, A. Temperature-associated increases in the global soil respiration record. *Nature* **464**, 579–582 (2010).
60. Zhao, J. et al. Intensified inundation shifts a freshwater wetland from a CO_2 sink to a source. *Glob. Change Biol.* **25**, 3319–3333 (2019).
61. Peichl, M. et al. A 12-year record reveals pre-growing season temperature and water table level threshold effects on the net carbon dioxide exchange in a boreal fen. *Environ. Res. Lett.* **9**, 55006 (2014).
62. Peng, Z. & Peng, G. Suitability mapping of global wetland areas and validation with remotely sensed data. *Sci. China Earth Sci.* **57**, 2883–2892 (2014).
63. Zhang, B. et al. Methane emissions from global wetlands: an assessment of the uncertainty associated with various wetland extent data sets. *Atmos. Environ.* **165**, 310–321 (2017).
64. Gumbricht, T. et al. An expert system model for mapping tropical wetlands and peatlands reveals South America as the largest contributor. *Glob. Change Biol.* **23**, 3581–3599 (2017).
65. *ERA5 Monthly Averaged Data on Pressure Levels from 1979 to Present* (ECMWF, 2020); https://doi.org/10.24381/cds.6860a573
66. *FAOSTAT Emissions Database* (FAO, 2020); http://www.fao.org/faostat/en/#data/GT
67. Qiu, C. et al. Large historical carbon emissions from cultivated northern peatlands. *Sci. Adv.* **7**, eabf1332 (2021).
68. Frolking, S., Roulet, N. & Fuglestvedt, J. How northern peatlands influence the Earth's radiative budget: sustained methane emission versus sustained carbon sequestration. *J. Geophys. Res. Biogeosci.* **111**, G01008 (2006).
69. Neubauer, S. C. & Megonigal, J. P. Moving beyond global warming potentials to quantify the climatic role of ecosystems. *Ecosystems* **18**, 1000–1013 (2015).
70. Matthews, E. & Fung, I. Methane emission from natural wetlands: global distribution, area, and environmental characteristics of sources. *Glob. Biogeochem. Cycles* **1**, 61–86 (1987).
71. Melton, J. R. et al. Present state of global wetland extent and wetland methane modelling: conclusions from a model inter-comparison project (WETCHIMP). *Biogeosciences* **10**, 753–788 (2013).
72. Papa, F. et al. Interannual variability of surface water extent at the global scale, 1993–2004. *J. Geophys. Res. Atmos.* **115**, D12111 (2010).
73. Junk, W. J. et al. Current state of knowledge regarding the world's wetlands and their future under global climate change: a synthesis. *Aquat. Sci.* **75**, 151–167 (2013).
74. Schroeder, R. et al. Development and evaluation of a multi-year fractional surface water data set derived from active/passive microwave remote sensing data. *Remote Sens.* **7**, 16688–16732 (2015).
75. Vanessa, R. et al. A global assessment of inland wetland conservation status. *Bioscience* **6**, 523–533 (2017).
76. Davidson, N. et al. Global extent and distribution of wetlands: trends and issues. *Mar. Freshw. Res.* **69**, 620–627 (2018).
77. *ArcWorld 1:3 M. Continental Coverage* (ESRI, 1992); http://www.oceansatlas.org/subtopic/en/c/593/
78. *Digital Chart of the World 1:1 M* (ESRI, 1993); https://www.ngdc.noaa.gov/mgg/topo/report/s5/s5Avii.html
79. *Global Wetlands* (UNEP-WCMC, 1993); https://www.arcgis.com/home/item.html?id=105a402642e146eaa665315279a322d1
80. Moreno-Mateos, D. et al. Structural and functional loss in restored wetland ecosystems. *PLoS Biol.* **10**, e1001247 (2012).
81. *Ramsar COP12 DOC.8* Report of the Secretary General to COP12 on the Implementation of the Convention (Ramsar Convention Secretariat, 2015).
82. Page, S. E. et al. Peatlands and global change: response and resilience. *Annu. Rev. Environ. Resour.* **41**, 35–57 (2016).
83. Swindles, G. T. et al. Widespread drying of European peatlands in recent centuries. *Nat. Geosci.* **12**, 922–928 (2019).

Acknowledgements

We thank many individuals for measuring and providing in situ GHG net fluxes from wetlands. This study was supported by the National Natural Science Foundation of China (grant no. 42071022), the start-up fund provided by the Southern University of Science and Technology (grant no. 29/Y01296122) and the High-level Special Funding of the Southern University of Science and Technology (grant no. G02296302). Jin Wu was supported in part by the Innovation and Technology Fund (funding support to State Key Laboratories in Hong Kong of Agrobiotechnology) of the HKSAR, China. D.C. was supported by Swedish National Strategic Research Programs: Biodiversity and Ecosystem Services in a Changing Climate (BECC) and Modelling the Regional and Global Earth system (MERGE). P.C. acknowledges support from the CLAND Convergence Institute 16-CONV-0003.

Author contributions

J.Z. and Z. Zeng designed the research; J.Z. performed the analysis; J.Z., Z. Zeng and A.D.Z. wrote the draft. J.Z., A.D.Z., D.C., G.M., P.C., X.J., C.Z., Jie Wu, Jin Wu, Z.L., X.H., L.E.B., J.H., Z. Zhang, S.J.R., A.C. and Z. Zeng contributed to the interpretation of the results and the writing of the paper.

Competing interests

The authors declare no competing interests.

Additional information

Extended data is available for this paper at https://doi.org/10.1038/s41561-022-00989-0.

Supplementary information The online version contains supplementary material available at https://doi.org/10.1038/s41561-022-00989-0.

Correspondence and requests for materials should be addressed to Zhenzhong Zeng.

Peer review information *Nature Geoscience* thanks Scott Bridgham and Debjani for their contribution to the peer review of this work. Primary Handling Editor: Tom Richardson, in collaboration with the *Nature Geoscience* team.

Reprints and permissions information is available at www.nature.com/reprints.

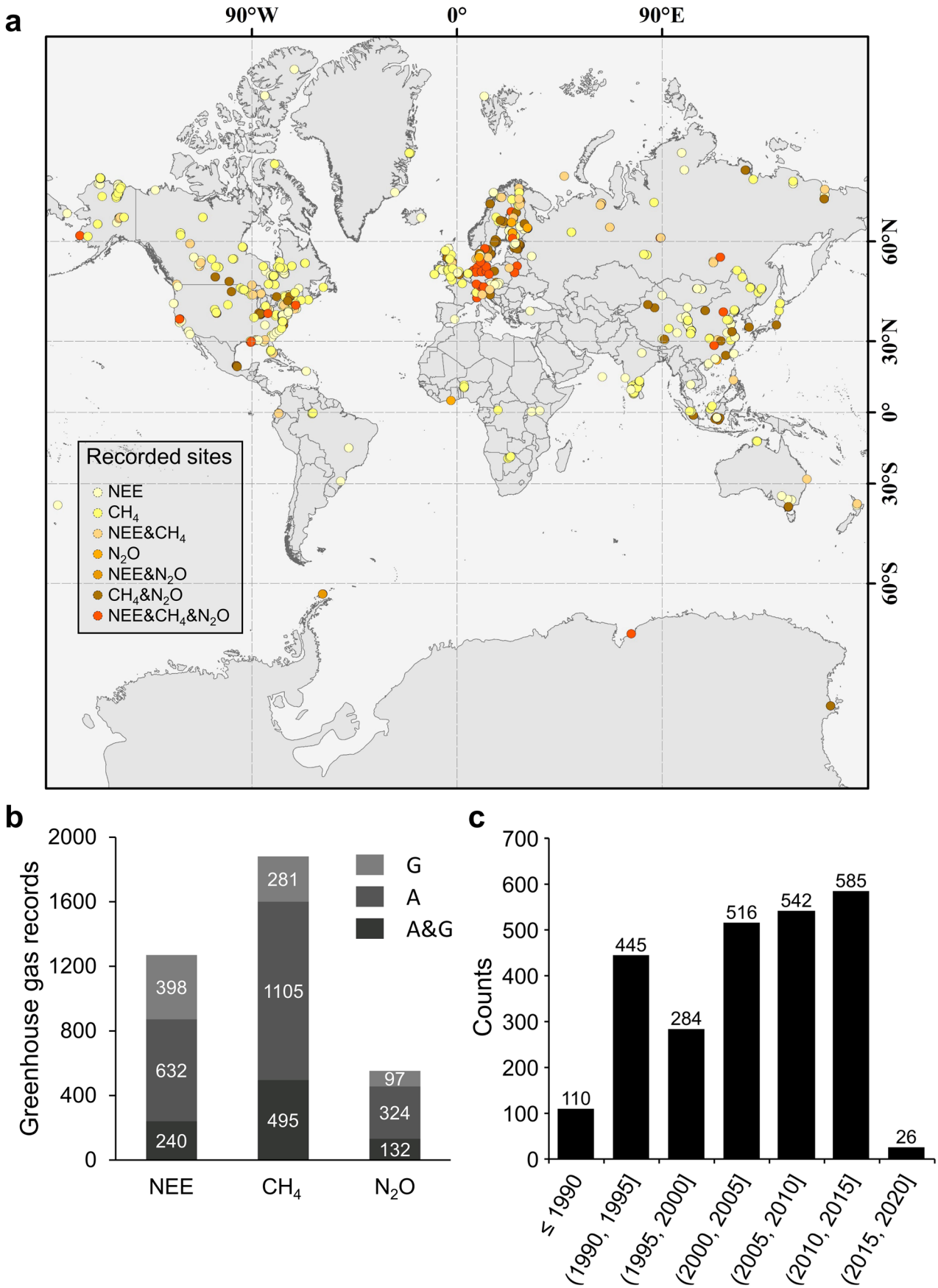

Extended Data Fig. 1 | The database of global, in-situ, greenhouse gas (GHG) exchange reports for wetlands. a, GHG data records from global wetlands. NEE, net ecosystem productivity; CH_4, methane flux; N_2O, nitrous oxide flux. **b**, Data entry. G, growing season; A, annual; G&A, growing season and annual. **c**, Year distribution of data source.

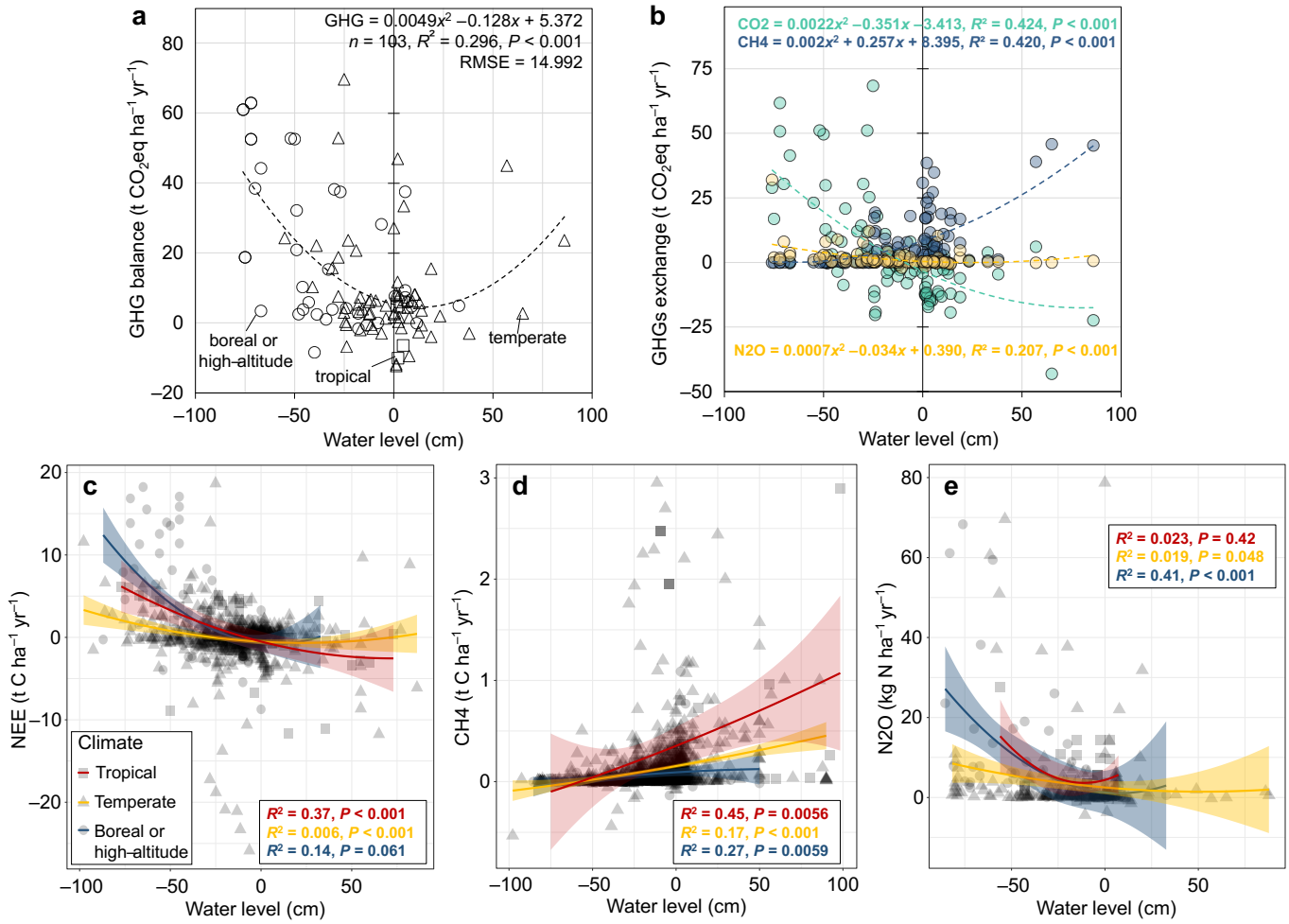

Extended Data Fig. 2 | Annual GHG flux values versus water level in wetlands. a, GHG balance, the nonlinear trend is formed by 103 site-year records reporting exact water levels and complete data including three major GHGs. **b**, CO_2, CH_4 and N_2O exchange. NEE (**c**), CH_4 (**d**) and N_2O (**e**) exchange across climate regimes with significant differences. The numbers of records for NEE, CH_4 and N_2O are 777, 1,247 and 294, respectively. Significant differences in panels **a** and **b** are based on the least square method with *F*-statistic, panels **c**–**e** are based on Spearman correlation analysis.

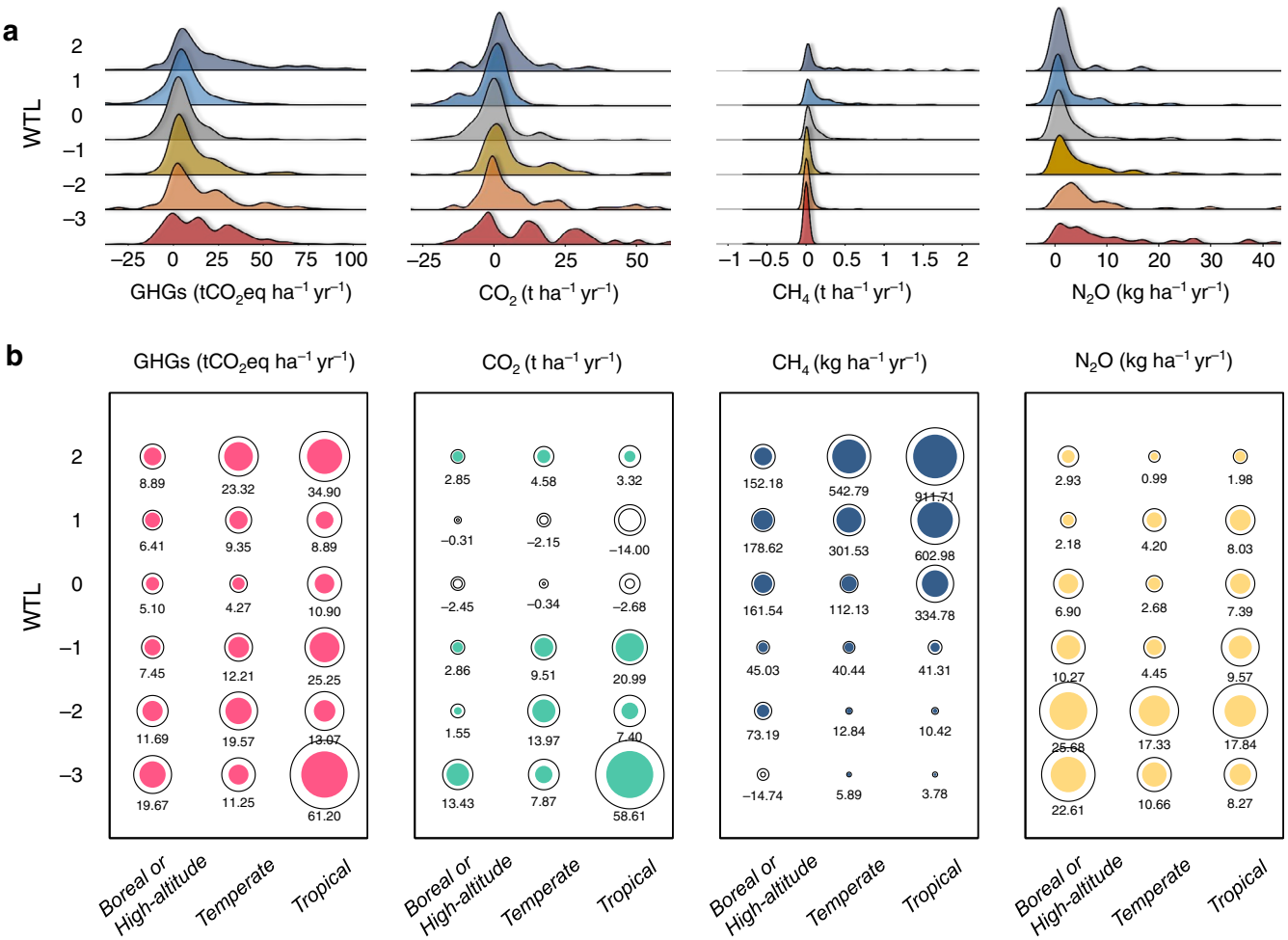

Extended Data Fig. 3 | The water-heat interaction impact on emissions of three greenhouse gases (CO_2, CH_4 and N_2O) and their sum. a, Frequency distribution of different greenhouse gases with WTL patterns. Note that *X* axes have been truncated for enhanced readability. **b**, GHG net exchange with hydrothermal patterns. The area of circles and rings represent the mean and 1.96SEs, respectively. The hollow circles represent absorption.

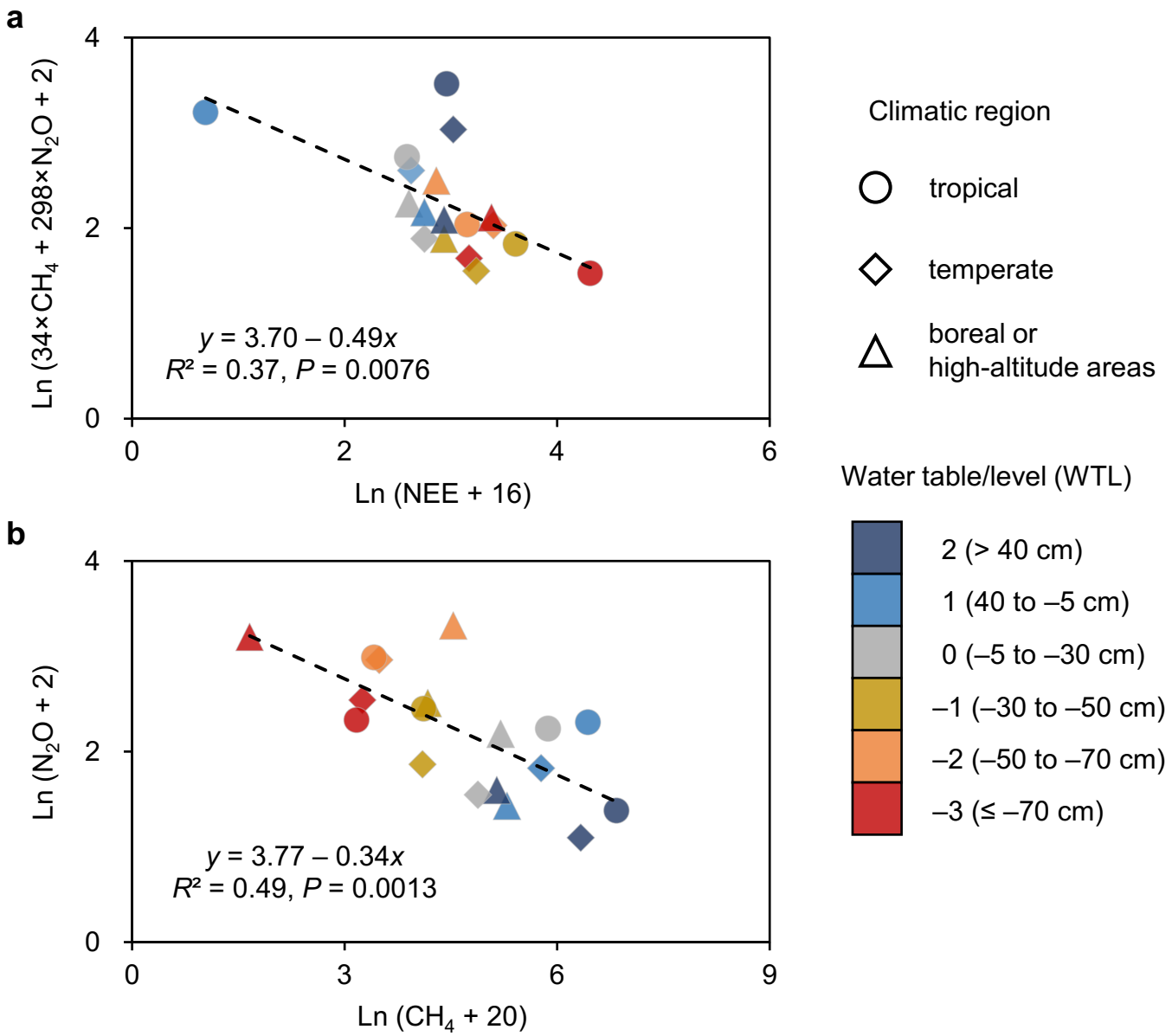

Extended Data Fig. 4 | The relationships of NEE versus the sum of CH_4 and N_2O (a), and CH_4 versus N_2O (b). To make the natural log transformations for visualization, we add the net exchange rates of GHGs to the diverse constants. The units of NEE, CH_4 and N_2O are t CO_2 ha^{-1} yr^{-1}, kg CH_4 ha^{-1} yr^{-1} and kg N_2O ha^{-1} yr^{-1}, respectively.

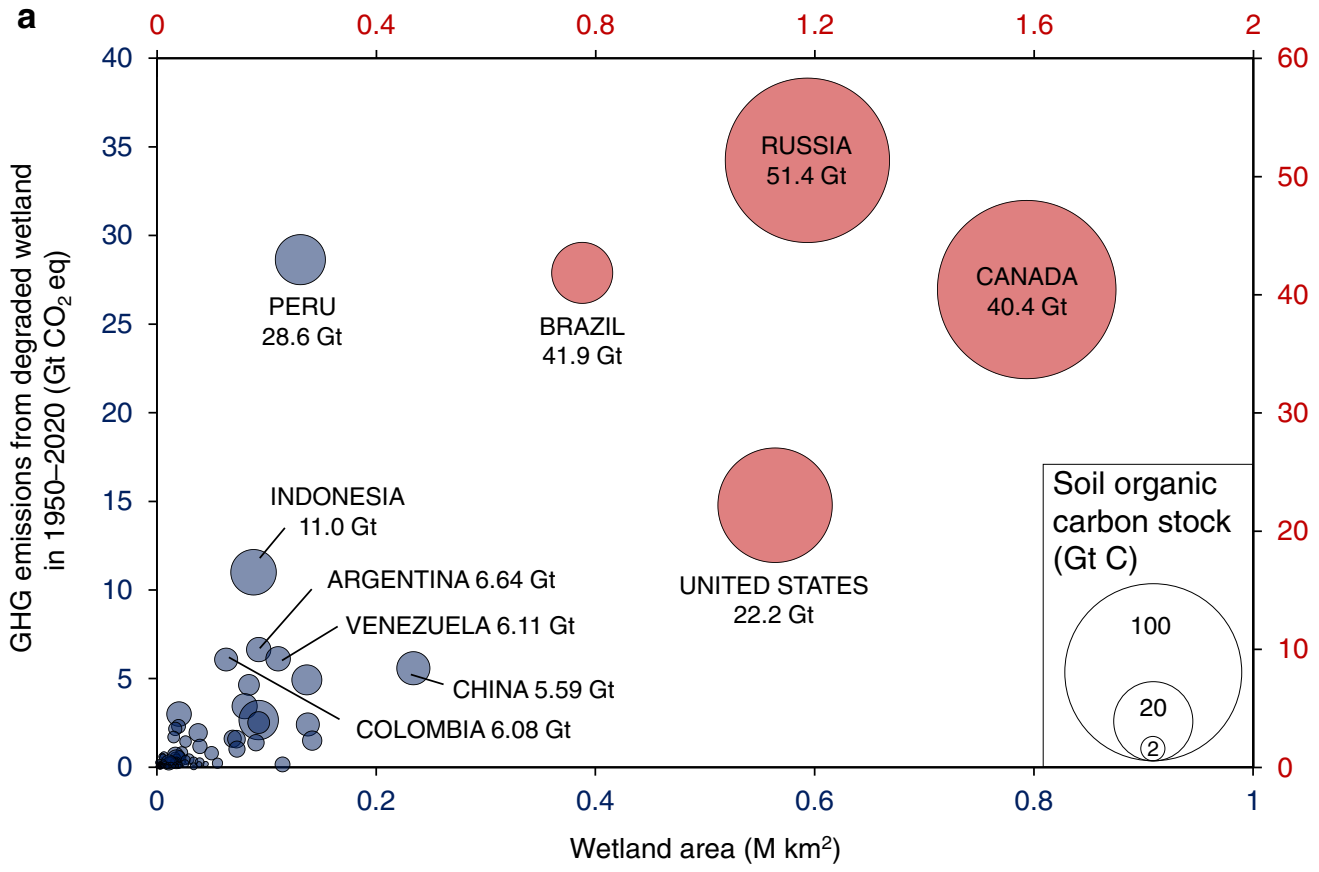

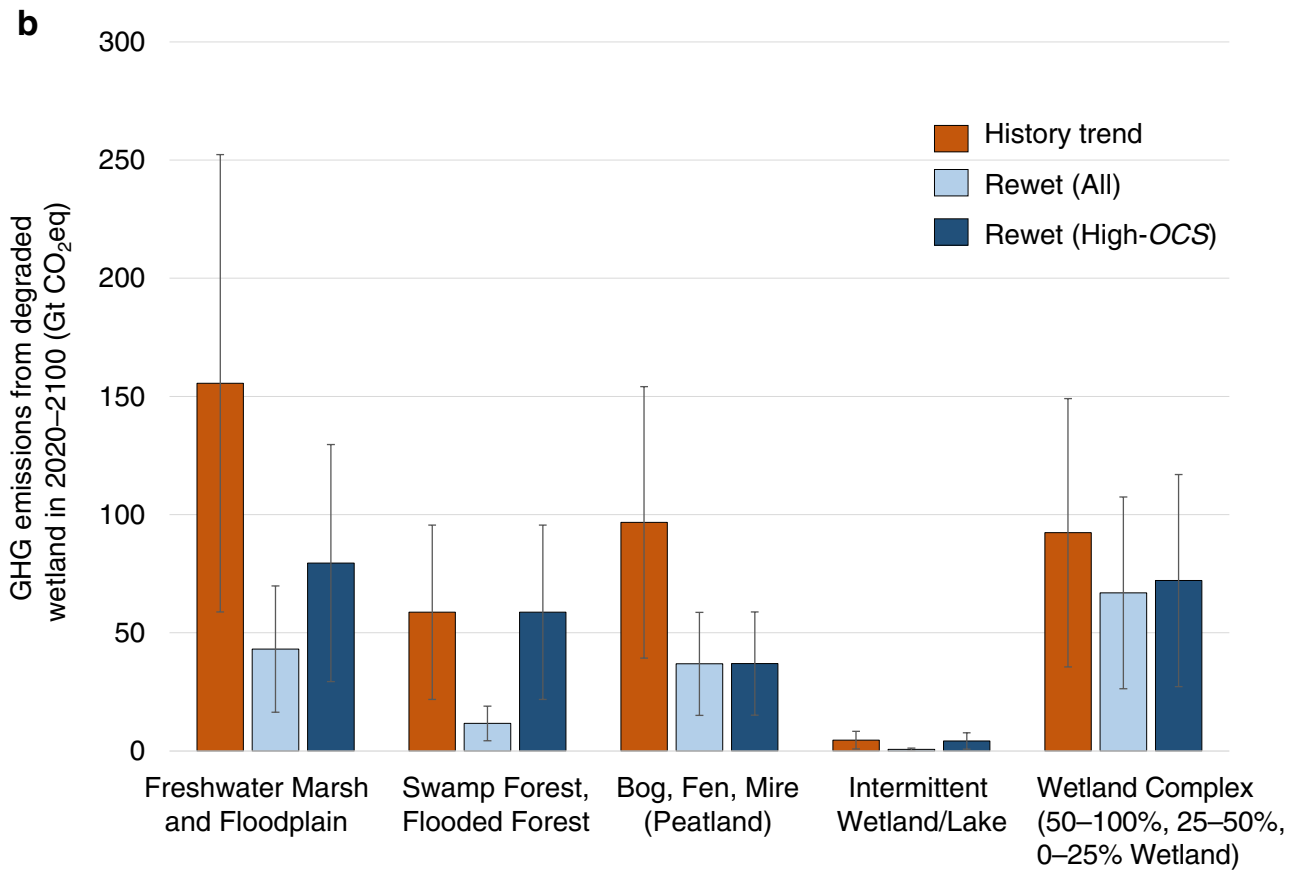

Extended Data Fig. 5 | See next page for caption.

Extended Data Fig. 5 | Greenhouse gas emissions from degraded wetlands in countries (a) and wetland categories (b). a, The country's historical emissions. The color of each circle corresponds to the axis of the same color (red/right; blue/left). The size of a circle represents the amount of soil organic carbon stock. **b**, Emissions from different wetland types under three scenarios. For details see Supplementary Data 1.

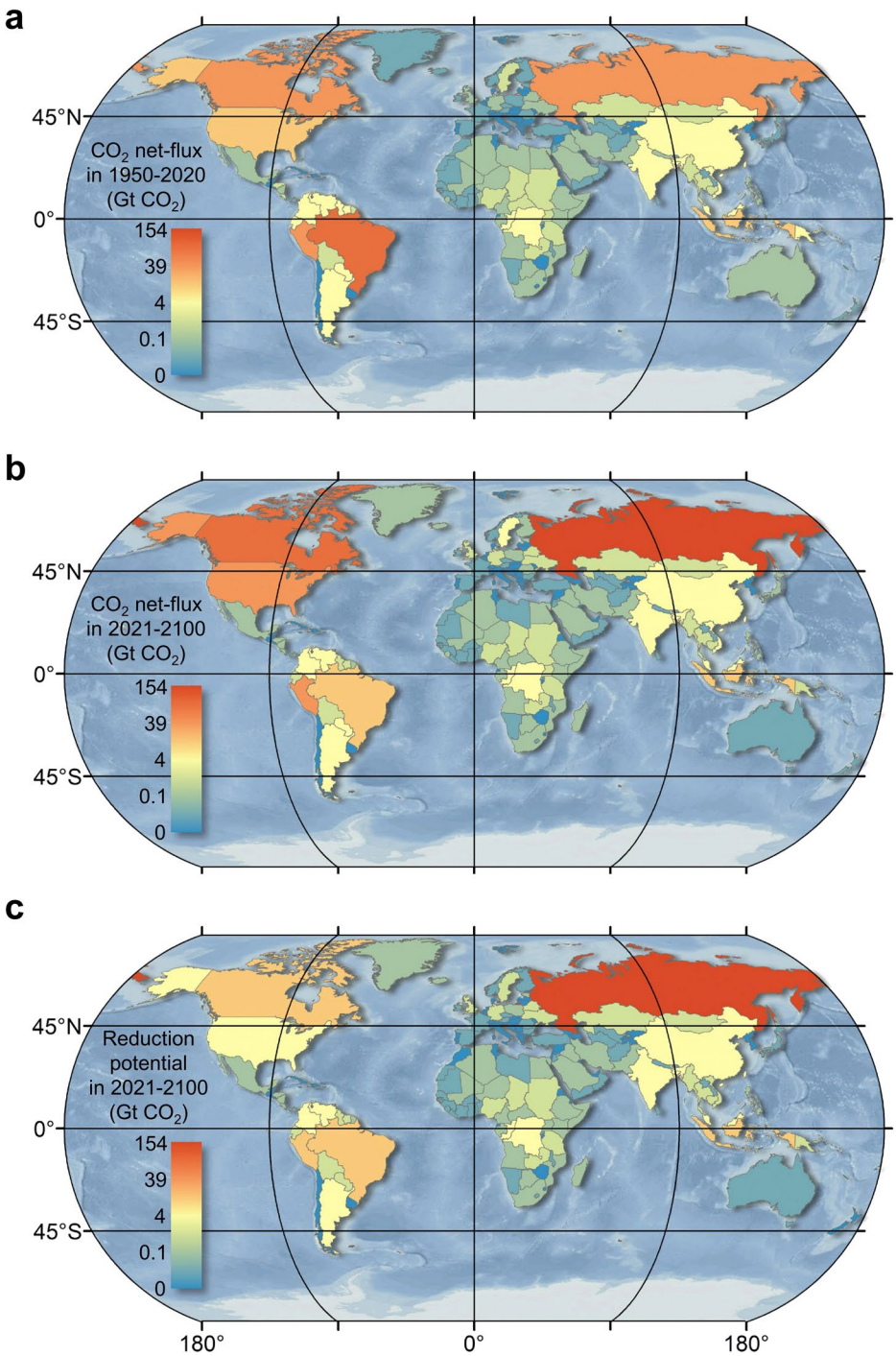

Extended Data Fig. 6 | Spatial pattern of the CO_2 emissions owing to wetland degradation (a, b) and reduction potential via rewetting wetlands (c). CO_2 emissions under history-derived scenario in 1950–2020 (**a**) and 2021–2100 (**b**). **c**, The reduction potential in 2021–2100 under the scenario of rewetting all degraded wetlands.

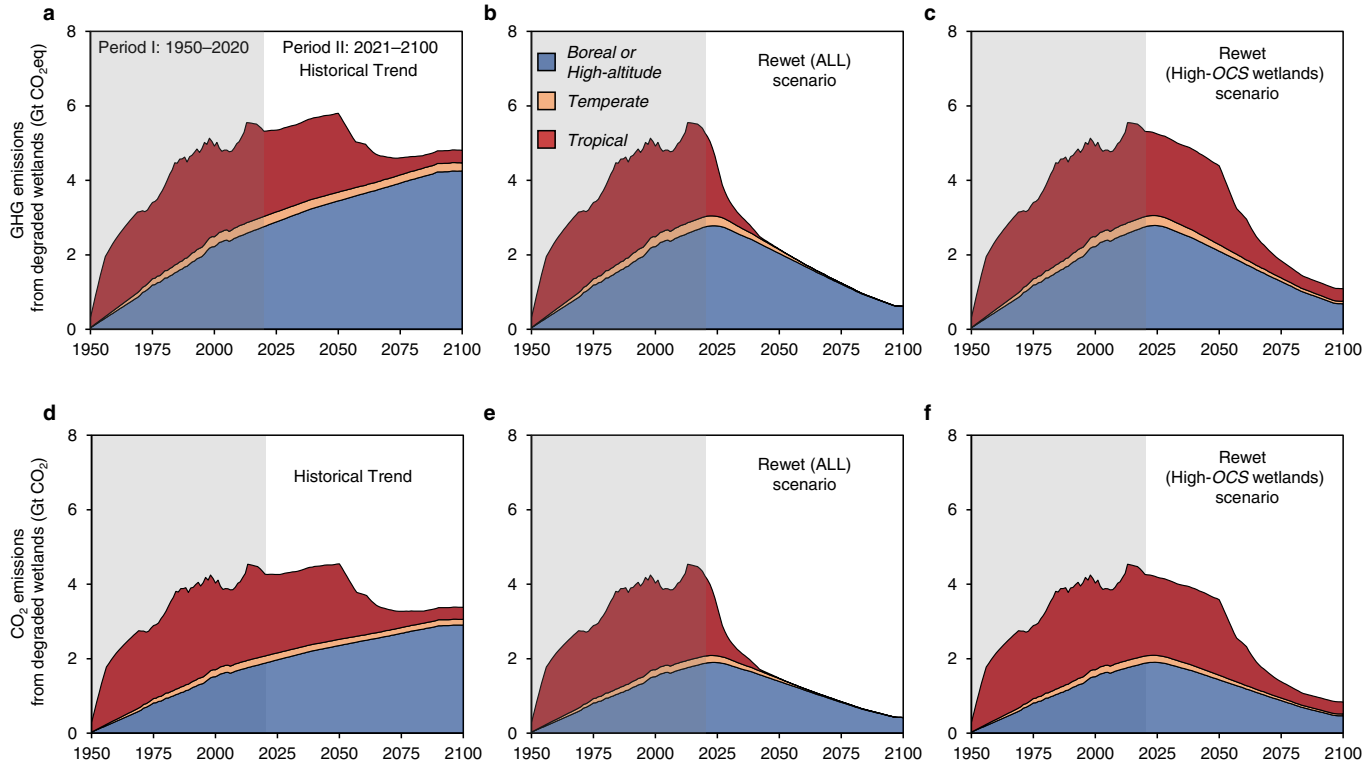

Extended Data Fig. 7 | Greenhouse gas emissions from degraded wetlands in three climatic zones under three scenarios. The sum of three greenhouse gas emissions (**a**–**c**) and CO_2 emissions alone (**d**–**f**). Period I is from 1950 to 2020 and period II is from 2021 to 2100. There are three scenarios in period II: the historical trend scenario (**a**, **d**), the scenario rewetting all degraded wetlands (**b**, **e**), and the scenario rewetting only high-OCS degraded wetlands (**c**, **f**).

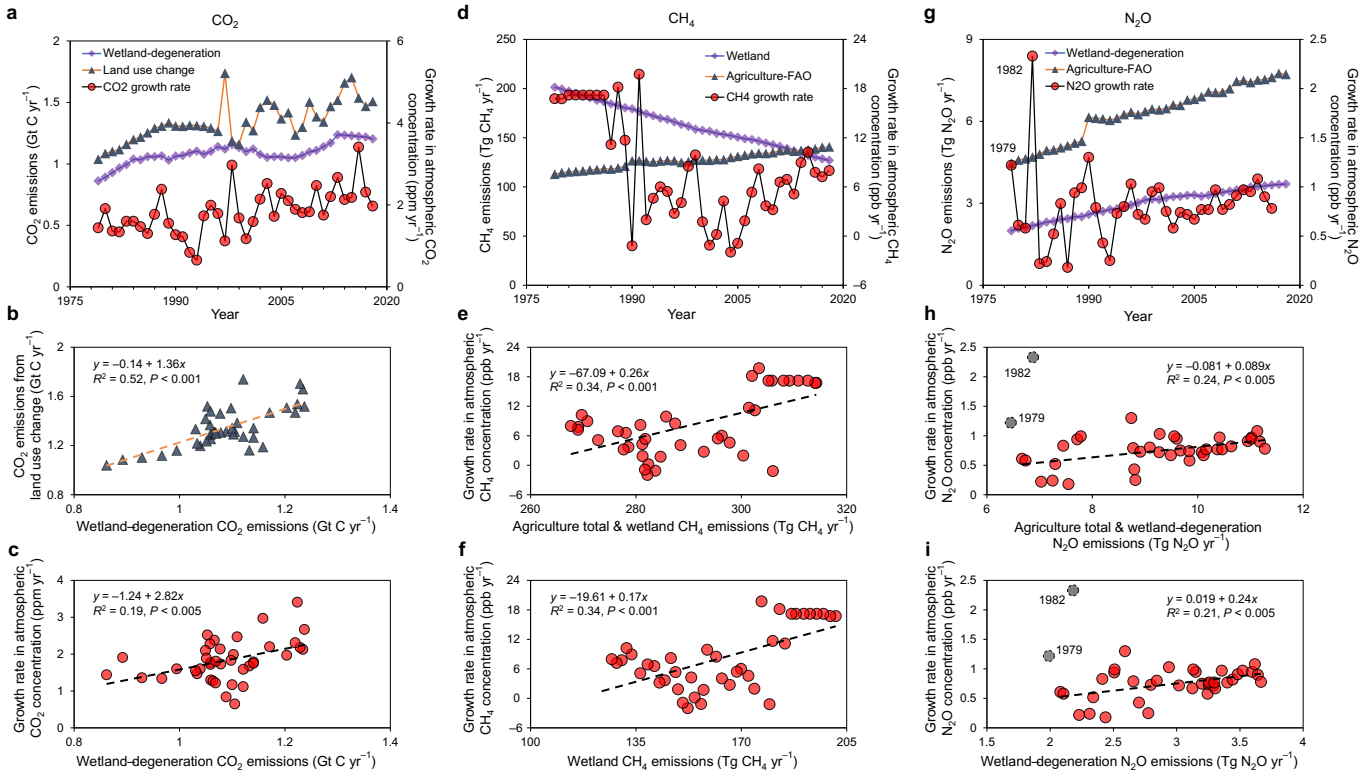

Extended Data Fig. 8 | Inter-annual atmospheric GHG concentration changes and emissions from wetlands and other major sources. a–i Data for CO_2 (**a**–**c**), CH_4 (**d**–**f**) and N_2O (**g**–**i**). Significant correlations exist between the flux of CO_2, CH_4 and N_2O from wetlands and their respective atmospheric concentration growth rates in the past three decades. In addition, the correlations persist when adding other major emission sources to wetlands. Note that atmospheric growth rates of N_2O for 1979 and 1982 are excluded.

Extended Data Table 1 | Wetland greenhouse gas (GHG) net fluxes in different climate regimes under various water table levels (WTL)

	Boreal		*Temperate*		*Tropical*	
WTL	**GHGs**	**95%CI**	**GHGs**	**95%CI**	**GHGs**	**95%CI**
2	8.89	4.82	23.32	10.45	34.90	18.78
1	6.41	2.24	9.35	5.56	8.89	16.89
0	5.10	4.36	4.27	2.46	10.90	14.37
-1	7.45	3.48	12.21	4.69	25.25	8.20
-2	11.69	9.38	19.57	11.45	13.07	19.39
-3	19.67	11.34	11.25	13.18	61.20*	38.50*

unit: $tCO_2eq\ ha^{-1}\ yr^{-1}$; * data from J. Leifeld *et al.*, 2019 (ref. 19).

Extended Data Table 2 | Wetland characteristics and GHG emissions for each continent

Continent	Area (million km²)	*OCS** (Gt C)	GHG net-flux from degraded wetland (Gt CO_2eq)			
			1950-2020 discharged	2021-2100 projected from historical trend	2021-2100 rewetting all wetlands scenario	2021-2100 rewetting high OCS wetlands scenario
Europe	1.27	99.51	53.94 ± 32.66 (68.38%)†	199.70 ± 120.69 (68.38%)	66.11 ± 39.93 (68.37%)	66.40 ± 40.26 (68.39%)
North America	2.71	158.81	62.64 ± 40.67 (70.19%)	100.77 ± 61.55 (68.69%)	75.05 ± 45.28 (68.41%)	78.25 ± 48.36 (68.79%)
Latin America	1.37	31.05	104.15 ± 65.83 (95.62%)	52.39 ± 33.17 (95.57%)	9.95 ± 6.31 (95.50%)	52.39 ± 33.17 (95.57%)
Asia & Oceania	1.23	26.88	36.07 ± 23.96 (89.83%)	35.70 ± 23.93 (89.03%)	6.17 ± 4.22 (87.34%)	35.08 ± 23.32 (89.38%)
Africa	1.08	13.23	19.64 ± 12.37 (95.73%)	19.30 ± 12.18 (95.67%)	1.87 ± 1.18 (95.52%)	19.30 ± 12.18 (95.67%)
Total	7.66	329.48	276.44 ± 175.49 (83.80%)	407.87 ± 251.51 (75.05%)	159.14 ± 96.92 (71.14%)	251.42 ± 157.28 (79.20%)
Reduction					248.72 ± 154.59 (77.55%)	156.44 ± 94.23 (68.37%)

*: *OCS* represents organic carbon stocks in soil layers from zero to one meter deep. †: The figures in the parentheses indicate the percentage of CO_2 emissions.

The figures in the parentheses indicate the percentage of CO_2 emissions, *OCS* represents organic carbon stocks in soil layers from zero to one meter deep.